Morphology of Colombian Emerald: Some Less Common Cases and Their Growth and Dissolution History

Karl Schmetzer and Gérard Martayan

The morphology of Colombian emerald, including growth and dissolution features of their faces, gives insight into growth and post-growth history of individual crystals. A collection of 15 isolated crystals and seven emeralds in matrix was studied by optical methods. The authors observed layered growth of prismatic, dipyramidal, and basal sectors that leads to crystals with prismatic to columnar or rarely pyramidal habit. In the latter case, prismatic growth sectors were not developed. The visual appearance of the crystal faces at the surface was influenced by etch patterns with the formation of cavities, pits, pointed hillocks, and stepped grooves, followed occasionally by layered overgrowth. Skeletal growth led to the formation of cavities in crystals, some of them resembling empty cups with planar bottoms. In these crystals, the basal faces showed indentations or deep cavities, surrounded by shells or rims of emerald, bound on both vertical surfaces by prism or dipyramidal faces. Emeralds in the form of slightly conical empty tubes also belong to the latter group. Possible relationships to trapiche emeralds and samples exhibiting the *gota de aceite* effect are discussed.

In general, the morphology of Colombian emerald originating from different mines is rather simple and formed by a small number of external crystal faces. We observe two dominant planes, the basal pinacoid and the first-order hexagonal prism, occasionally in combination with small second-order hexagonal prism faces and first- and/or second-order hexagonal dipyramids (Goldschmidt, 1913; Schwarz and Giuliani, 2002; Moore and Wilson, 2016). The internal growth pattern of such samples, which normally show prismatic habit, consists of growth planes parallel to the external crystal faces (Kiefert and Schmetzer, 1991).

Occasionally, natural emerald and beryl crystals show etching and dissolution features (an overview of the pertinent literature is given in box A). Other growth features are due to skeletal and polygonal growth of beryl crystals (see box B). Both growth features are related to the observations made in this article for Colombian emerald crystals.

Rarely mentioned are emerald crystals with conical habit (Johnson, 1961a,b)—or *vasos* in the form of slightly conical empty tubes (Klein, 1941)—or emeralds in the form of prismatic, empty "cups" with planar bottoms (Weldon et al., 2016). In most references, such emeralds with conical habit (figure 1) or emerald vasos or cups (figure 2) have been briefly mentioned or have only been pictured without considering a possible growth mechanism. In the following discussion, we will use only the term "cups" for both slightly different variants.

In Brief

- The surface texture of Colombian emerald crystals reveals details about growth and post-growth history.
- Several crystals show indications of natural etching in aggressive fluids, and some samples have undergone several subsequent growth and corrosion steps.
- In crystals with a conical shape, only basal and dipyramidal growth sectors were developed.
- Skeletal growth is observed in emeralds showing the form of empty cups or emeralds with indentations on the basal face.
- Within the empty cups, polygonal growth of small emerald columns is observed.

See end of article for About the Authors and Acknowledgments.
Gems & Gemology, Vol. 59, No. 1, pp. 46–71,
http://dx.doi.org/10.5741/GEMS.59.1.46

Figure 1. This Colombian emerald (sample 10, 25.0 mm in length) shows conical habit in the upper part and prismatic habit in the lower part; the base is covered with numerous pointed hillocks. Photo by G. Martayan.

Box A: Literature on Dissolution Features of Beryl and Emerald Crystals

Etch pits on basal, prismatic, and pyramidal faces of Colombian emerald have been described or depicted by a few authors (e.g., Honess, 1917, 1929; Medina et al., 1983; Moore and Wilson, 2016). Considering the mineral beryl in general, various forms of tiny cavities or pits have been observed with different shapes reflecting the symmetry of the individual basal, prismatic, or dipyramidal crystal faces (figure A-1). In addition, the shape of etch patterns varies between samples from different localities (Kurumathoor and Franz, 2018). It has also been mentioned that while some faces of crystals might show etch pits, other faces of the same crystal are completely free of such textures (Petersson, 1889; Arzruni, 1894; Vrba, 1895; Tschermak, 1897; Kohlmann, 1908; Sinkankas, 1981).

These generally observed features of etch patterns in beryls from numerous localities are consistent with the results of etching experiments performed in the laboratory (Taube, 1895/1896; Feklichev, 1963). Such experimental processes were done in various acidic or basic solutions, but normally only for periods of seconds to minutes.

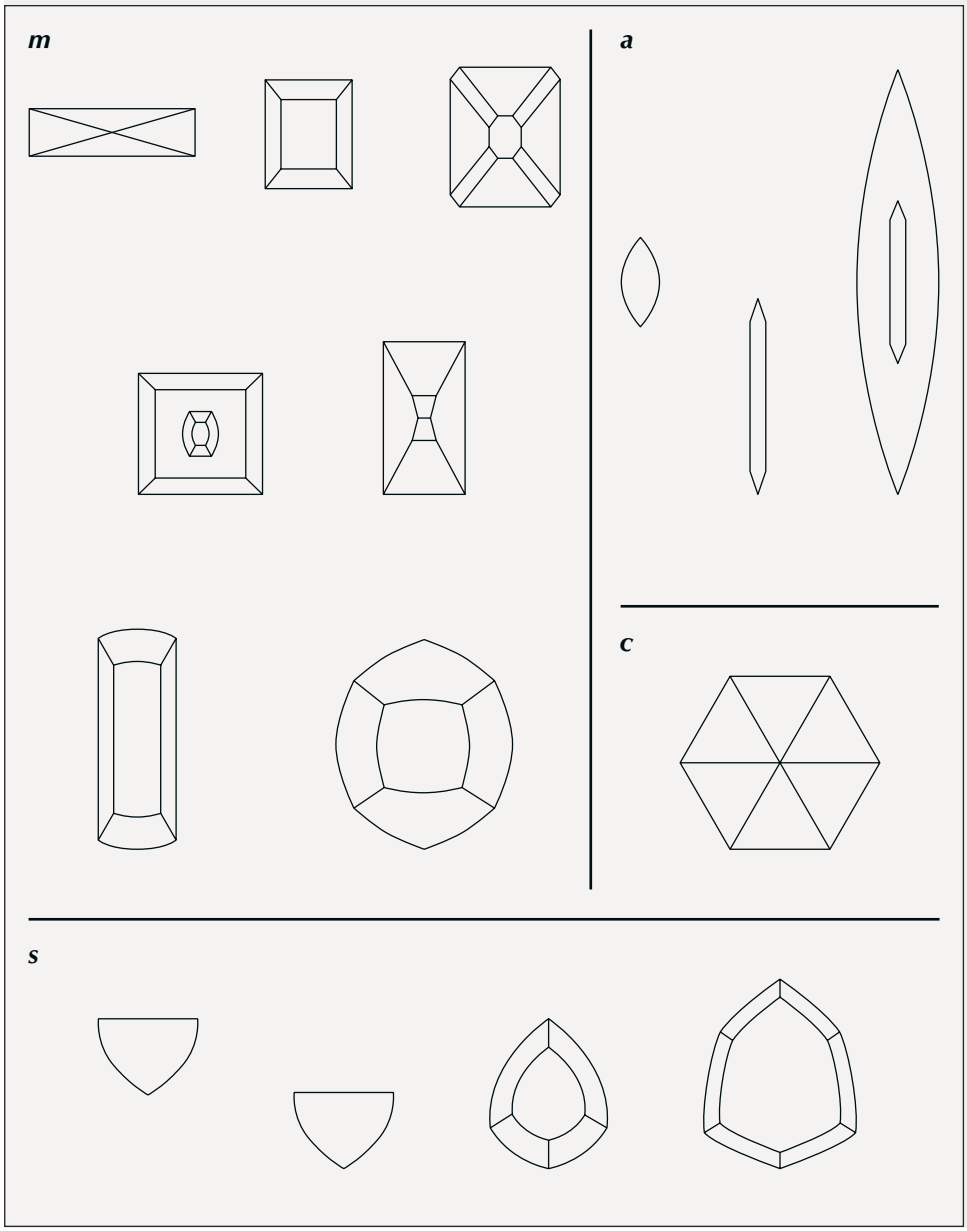

Figure A-1. Shape of etch pits observed optically on prismatic m *and* a *faces, on the basal pinacoid* c *and on dipyramidal* s *faces of numerous beryl crystals from Brazil. After Kohlmann (1908).*

Examination at high magnification by optical and electron microscopy reveals that the patterns of variously shaped cavities developed by natural or artificial etching show stepped surfaces of various forms (Scandale et al., 1990; Sunagawa and Urano, 1999; Sunagawa, 2003; Demianets et al., 2006; Dem'yanets and Ivanov-Schitz, 2009; Kurumathoor and Franz, 2018).

All these observations, however, are different from the effects of heavy dissolution, in which the crystals' original surfaces are completely or partially dissolved, forming more or less deep cavities or grooves (Ford, 1906; Zedlitz, 1941; Bartoshinsky et al., 1969; Koivula, 1981; Lyckberg et al., 2009; Tempesta et al., 2011). Such heavy resorption has been mentioned for beryl from specific localities—e.g., California, Brazil, or Ukraine (figure A-2)—and it has also been shown for emerald from Colombia (figure A-3, left).

Furthermore, it should be mentioned that heavy etching can produce pointed forms consisting of single or multiple tapering tips representing the residue of the former as-grown basal plane (figure A-3, right; see Penfield and Sperry, 1888; Penfield, 1890; Lacroix, 1896; Sunagawa, 2005; Moore and Wilson, 2016). This feature is also seen in the heavily etched Colombian emerald shown in figure A-3, left.

Figure A-2. Yellow and greenish yellow beryl crystals from the Volodarsk mining area in Ukraine showing heavily dissolved surface patterns due to natural etching and dissolution subsequent to the crystal growth process. Crystal length: 61 mm (left) and 43 mm (right). Photos by Peter Lyckberg.

Figure A-3. Left: A heavily etched Colombian emerald crystal from Muzo measuring 27 mm in length. The basal pinacoid is completely dissolved, leading to numerous pointed hillocks; the growth sectors related to the a *prism faces are optically reflective. Photo by Jeff Scovil. Right: Etched beryl crystal from Pont de Barost, Haute-Vienne, France, showing a completely dissolved basal face with numerous pointed hillocks. From Lacroix (1896).*

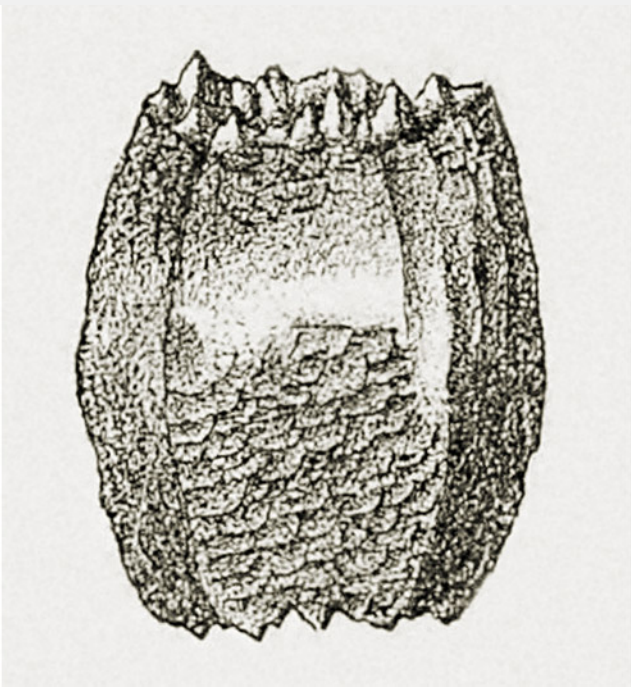

BOX B: LITERATURE ON SKELETAL AND POLYGONAL GROWTH OF BERYL CRYSTALS

From the literature, beryls with hexagonally outlined rims or walls are known from different pegmatites. Within these main walls, highly variable, irregularly shaped to hexagonally outlined areas of beryl are found, with other pegmatite minerals filling the remaining space (figure B-1). These beryls, designated as "skeletal" or "shell" crystals, mostly consist of a rim or shell enclosing additional beryl shells or rims and other pegmatite minerals (Hunt, 1892; Shaub, 1937; Johnston, 1945; Norton et al., 1962; Beus, 1966; Sinkankas, 1981). It is not mentioned in the works cited whether the beryl inside the dominant surrounding wall represents parts of a single crystal, connected to the main wall or rim, or independent individual crystals.

From the viewpoint of crystal growth, in skeletal crystals with incomplete planes, crystal edges grow in favor of plane faces (Sunagawa, 1981, 1999). This is of course dependent on the growth environment. In the flux synthesis of emerald, for example, it is possible to grow skeletal crystals with depressions of the *m* prism face (Oishi et al., 1994).

On the other hand, the polygonal growth of small beryl columns on a basal plane of a larger crystal and the subsequent overgrowth of this structure by later generations of beryl was described by Sahama (1966) and is shown in figure B-2.

Visually, a beryl crystal depicted by Hills (1890) and shown in figure B-3, seems to show both growth features: skeletal and polygonal growth. In this sample, we observe a rim surrounding a larger cavity. Within this cavity, we observe irregular walls or columns, which end at different heights in the cavity with small crystal faces.

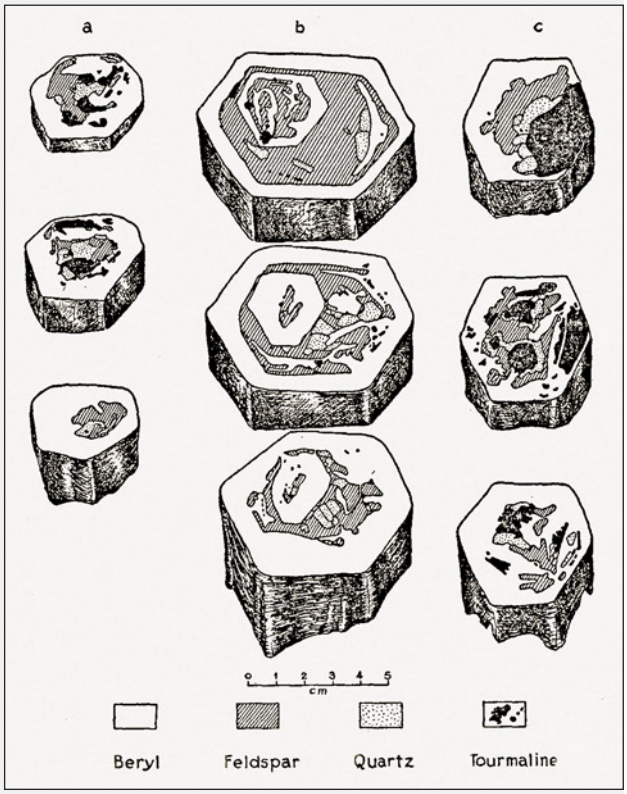

Figure B-1. Slices of three beryl crystals from Alto Cruzeiro, Paraíba, Brazil, with skeletal growth structure. Three slices were cut from each sample oriented perpendicular to the c*-axis. Within an outer skeletal rim or shell of beryl, further beryl crystals and other pegmatite minerals were observed. From Johnston (1945).*

Figure B-2. Sketch of a beryl crystal showing polygonal growth of small individual pyramidal beryl crystals ending in basal faces; this morphological structure is seen on the surface and within the crystal. In the latter case, this area was overgrown in subsequent growth steps. From Sahama (1966).

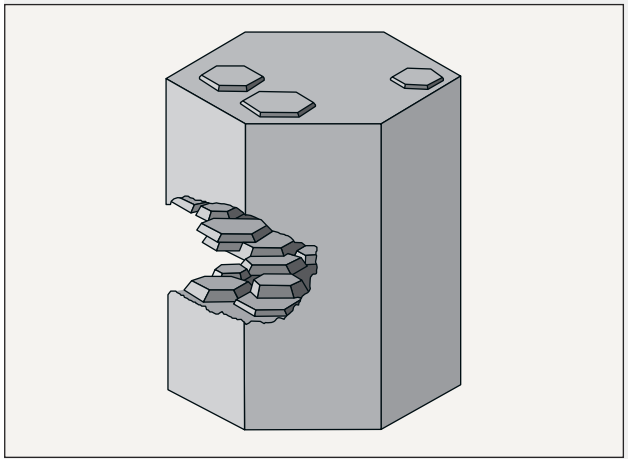

Figure B-3. Surface structure in a beryl from Mount Antero, Colorado, with a rim surrounding a larger cavity with irregular walls or columns developed within the cavity. From Hills (1890).

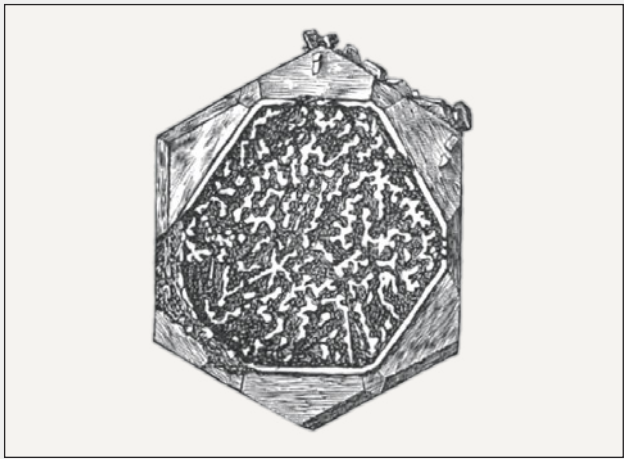

Figure 2. In sample 17 (26 mm in length), a base of black shale (not visible) is covered with numerous albite, calcite, and pyrite crystals. In this matrix, five emerald crystals are embedded, two of them developed in the form of empty cups. The emerald cup on the right is 5.5 mm long. Photo by G. Martayan.

Of commercial interest, in addition to facetable material without special structural properties, are samples with a fixed six-rayed pattern with or without a central core—designated "trapiche" emerald (Bernauer, 1926; Nassau and Jackson, 1970; Pignatelli et al., 2015; Schmetzer, 2019; Smith, 2021) or samples with an internal growth pattern named *gota de aceite* (Spanish for "drop of oil") (Gübelin, 1944; Bosshart, 1991; Ringsrud, 2008; Hainschwang, 2008; Schmetzer, 2009; Gao et al., 2017).

Some of the morphological features mentioned above, such as the various forms of the trapiche pattern, have been studied in detail to evaluate the growth mechanism. The *gota de aceite* effect has also been properly described, but its formation, either by dissolution (etching) or polygonal growth and, in both models, by subsequent overgrowth of the surfaces of the small hillocks or columnar crystals formed in the first step, is still a matter of discussion (Bosshart, 1991).

In a recent publication, Pignatelli et al. (2022) described several Colombian emeralds with unusual habits. According to their results, the growth mechanism of two emerald cups, one spongy emerald crystal, and one spear-shaped sample is mainly due to etching (post-growth dissolution), and the morphology of an emerald crystal with a horseshoe-shaped appearance is related to incomplete, nonuniform growth caused by mineral inclusions acting as growth obstacles.

The present paper tries to contribute to the understanding of these less common morphological and growth phenomena of Colombian emerald and offer descriptions and understanding of different patterns mentioned, especially by enlarging the database for such rare samples with remarkable morphological features. These samples provide a unique opportunity for investigation, but their rarity limits the investigation to nondestructive methods. In this way, the paper would further contribute to our understanding of the growth and post-growth history of Colombian emerald.

MATERIALS AND METHODS

The present study is based on examination of 15 isolated emerald crystals and seven specimens with emerald crystals in mineral assemblages with albite, calcite, dolomite, and pyrite on gray or black shales (table 1). All samples are from a private collection and were purchased within the last 20 years in Bogotá or near emerald mines in Colombia. This does not necessarily indicate that all samples were un-

TABLE 1. Properties of the examined emerald crystals.

Sample no. and locality	Matrix specimen dimensions (mm)	Emerald crystal dimensions (mm)[a]	Weight[b]	Crystal faces[c] and habit	Surface features of emerald crystals	Remarks	Figures
1: Chivor	Crystal on gray shale, 40 × 28	L 11.8, D 3.5	22.7 g	*c, m;* columnar	Growth steps on *m*	Associated minerals: dolomite, pyrite	4
2: La Pita	—	L 18.0, D 11.1–12.0	18.61 ct	*c, m, s;* columnar	Irregular openings in *c*, etch pits and grooves on *m*	Cavities below *c*, larger than the different openings	5
3: Chivor	Crystal on black shale, 41 × 30	L 23.6, D 5.1–15.5	21.4 g	*c, m, a, p, s;* elongated tabular	Irregular openings in *c*, partly deeply etched *m* growth sectors	Associated minerals: albite, pyrite, calcite	6
4: Coscuez	—	L 31.1, D 7.1–7.6	11.42 ct	*c, m, a;* columnar	Partly deeply etched *m* growth sectors; in other parts, growth steps on *m*	—	7
5: La Pita or Muzo	—	L 10.0, D 4.0	0.67 ct	*c;* conical	Growth striations on the sides of the pyramid	—	8, A and B
6: La Pita	—	L 8.8, D 2.0–2.1	0.33 ct	*c;* conical and prismatic part	Growth striations on both parts	—	8A
7: La Pita	—	L 8.8, D 2.5–2.8	0.46 ct	*c;* conical and prismatic part	Growth striations on both parts	—	8, A and C
8: Chivor	—	L 9.8, D 4.8–5.1	1.61 ct	*c, m, a, s, p;* partly conical with tabular part	Growth steps on conical surface and on *m* faces of the tabular part	Groth tubes along the *c*-axis in tabular part	9
9: Muzo (?)	—	L 20.8, D 10.8–12.1	10.76 ct	*c, m, a, s, p;* conical	Growth steps on *m*, finer structures on the conical part	Residual dark gray (carbonaceous) material in cavities	10
10: La Pita	—	L 25.0, D (top) 15.0–16.6, D (bottom) 9.5–13.0	35.87 ct	*m, a;* partly conical with columnar part	Growth steps, mainly parallel to *c*, *p* on conical surface; growth steps on *m* of the columnar part; hillocks on *c*	Extensions of growth sectors confined to the *a* prism	1 and 11
11: Chivor	Crystal on gray shale, 56 × 37	L 15.5, D 3.5–4.1	43.2 g	*c, m, a, u, p, s;* columnar	Indentations on *c*, growth steps on prismatic faces	Associated minerals: calcite, pyrite	12A
12: Chivor	Crystals on dark gray shale, 51 × 37	aggregate of 11 parallel crystals; largest L 12.5, D 5.0–6.5	50.0 g	*c, m, a;* columnar	Indentations on *c* of all crystals, growth steps on prismatic faces	Associated minerals: pyrite, dolomite, albite	12B and 13, A and D

earthed within this period or in the last few years—some of them might originate from Colombian collections, with samples being kept there for several years or even decades before they were offered for sale.

According to the general knowledge of emerald formation in the various Colombian deposits, all of the emeralds grew in cavities and were removed by the miners, either as isolated crystals or in matrix.

TABLE 1 (continued). Properties of the examined emerald crystals.

Sample no. and locality	Matrix specimen dimensions (mm)	Emerald crystal dimensions (mm)[a]	Weight[b]	Crystal faces[c] and habit	Surface features of emerald crystals	Remarks	Figures
13: Chivor	Crystals on gray shale, 44 × 29	Three aggregates of nine, eight, or three parallel crystals; largest L 16.5, D 6.5–7.5	31.1 g	*c, m, a;* columnar	Indentations on *c* of all crystals, growth steps on prismatic faces	Associated minerals: calcite, dolomite, albite, pyrite	12C and 13, B and C
14: Chivor	Crystal on black shale, 49 × 22	L 6.3, D 3.8–6.0	14.6 g	*c, m, a;* columnar	Deep indentations on *c*, growth steps on prismatic faces	Associated minerals: calcite, albite, pyrite	14
15: Chivor	—	L 37.4, D 6.6–7.1	17.24 ct	*c, m, a, i, f, k;* columnar	Deep indentations on *c*, growth steps on prismatic faces	Color zoning	15
16: Chivor	—	L 10.8, D 7.3–8.7	6.37 ct	*c, m, a, s, p;* columnar	Open cup, growth steps on prismatic faces	Irregularly shaped hillocks and columns in cup	16
17: Chivor	Five crystals on black shale; 26 long, 11–20 wide	cup 1: L 5.5, D 2.5–3.0 cup 2: D 3.0 crystal 1: L 12.0, D 2.0 crystals 2 and 3 are smaller crystal 3: L 3.8	4.5 g	*c, m;* columnar	Open cups, growth steps on *m*	Associated minerals: albite, calcite, pyrite; irregularly shaped hillocks and columns in both cups	2 and 17
18: Chivor	—	L 19.6, D 9.2–10.0	13.58 ct	*c, m, a, u, p, s;* columnar	Open cup, openings also in *p*, growth steps on prismatic faces	Irregularly shaped framework of walls in cup	18
19: Chivor	—	L 3.0 and 7.8, D 7.3–7.5	2.68 ct	*c, m, a, i, u p, s, f, k;* columnar	Half cup	Internal channels filled with fine-grained beryl	19
20: Chivor	—	L 13.0, D 3.5–4.5	1.96 ct	*c, m, p*	Partial cup	Pyrite at the bottom of the cavity, internal channels	20, left
21: Chivor	—	L 9.0, D 4.0–5.5	1.41 ct	*c, m, a*	Partial cup	Pyrite at the bottom of the cavity	20, right
22: Chivor	—	L 14.4, D 3.4–4.4	1.63 ct	*c, m, a;* elongated columnar, slightly conical	Etch pits and grooves on prismatic faces	Slightly conical tube along the *c*-axis through the complete crystal	21 and 22

[a]*L represents the length of the emerald crystal, D represents measurements of diameters between two* m *prismatic faces.*
[b]*Weights of samples with emerald crystals in matrix are given in grams; weights of isolated emerald crystals are given in carats.*
[c]*Based on a cell with* a:c *ratio of 1:0.996; basal pinacoid* c *{0001}, first-order hexagonal prism* m *{10$\bar{1}$0}, second-order hexagonal prism* a *{11$\bar{2}$0}, dihexagonal prism* i *{21$\bar{3}$0}, first-order hexagonal dipyramids* p *{10$\bar{1}$2} and* u *{10$\bar{1}$1}, second-order hexagonal dipyramids* s *{11$\bar{2}$2} and* f *{33$\bar{6}$2}, and dihexagonal dipyramid* k *{21$\bar{3}$1}.*

For the evaluation of growth history, it is important to look at all morphological features of a sample as a summary and not only at isolated crystal faces. The morphology of the samples was examined visually, and crystal faces were determined by goniometric measurements and/or by the measurement of angles between crystal faces in the microscope.

The samples were studied exclusively by nonde-

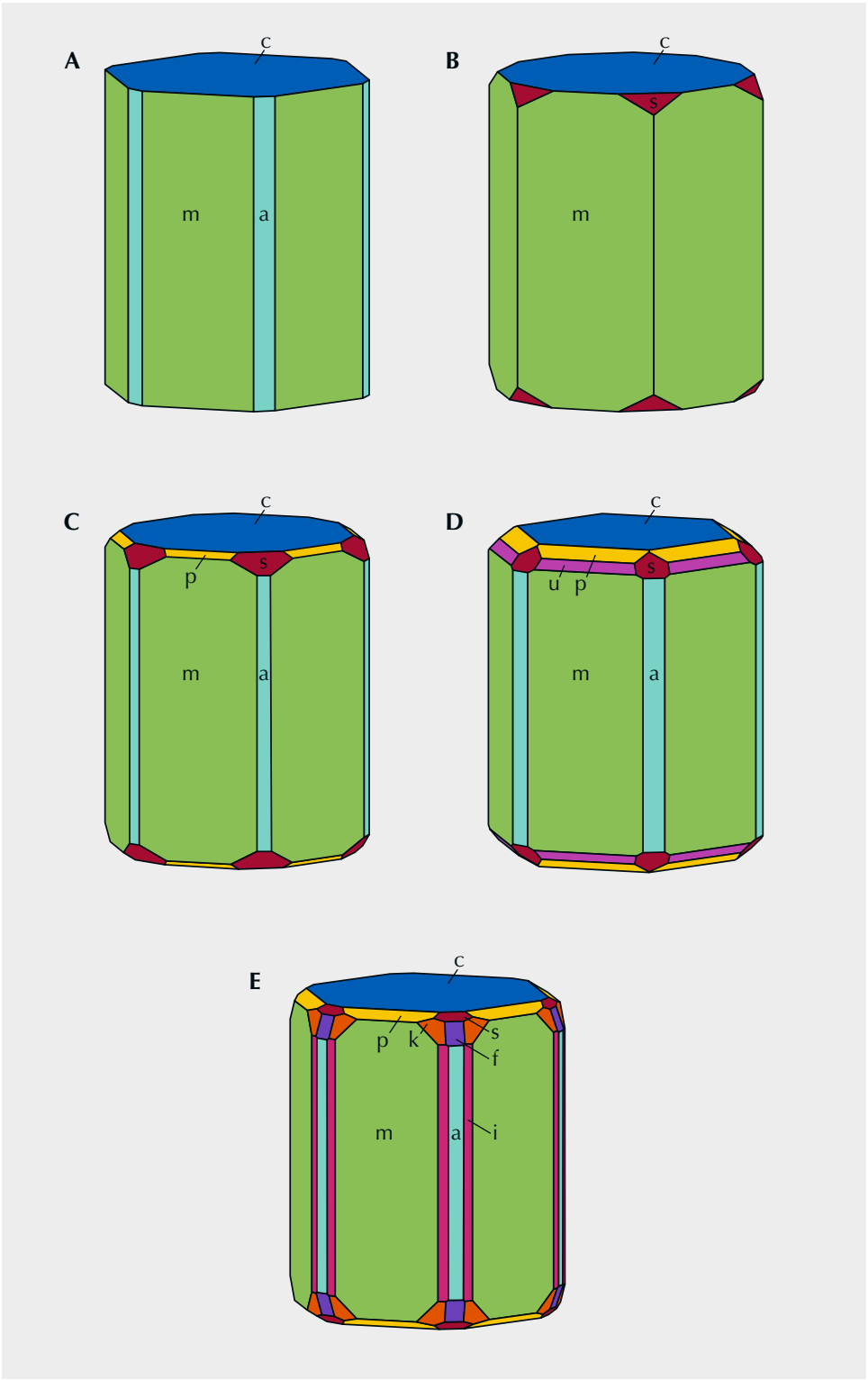

Figure 3. Morphology of Colombian emeralds observed in the present study. A–D: Most samples show dominant m *prism and basal* c *faces; occasionally we also observed smaller* a *prism faces in combination with* s, p, *and* u *hexagonal dipyramids. E: Furthermore, two of the crystals showed additional small* i *prism faces in combination with* f *and* k *dipyramids. Drawings by K. Schmetzer.*

structive methods, especially by optical microscopy at low magnification (up to 80×). A few transparent samples of appropriate size were also examined in immersion using benzyl benzoate as the immersion liquid. For such rare materials (isolated emerald crystals or matrix specimens), no destructive techniques (e.g., slicing or polishing of the crystals) could be applied nor any coating of the samples for an investiga-

tion at higher magnification in the scanning electron microscope.

In one sample, the identity of the substances filling the growth tubes was determined by a combination of X-ray diffraction (using a Bruker D8 Advance Eco X-ray diffractometer), energy-dispersive X-ray fluorescence (EDXRF, using a portable Bruker Tracer III-SD EDXRF analyzer), and Raman spectroscopy (using an Ahura First Defender portable Raman device). Part of the filling could be removed easily with a needle and was made available in that way for examination.

RESULTS AND DISCUSSION

General Aspects. Some general aspects of crystal morphology will be described first, which can help to characterize the individual samples.

Morphology. Most isolated emerald crystals were slightly distorted (e.g., with different diameters measured between opposite prisms) but with clearly defined faces. Nine of these crystals were columnar to prismatic, and six were conical, some of them with prismatically developed areas. The emeralds on six of the seven matrix samples showed columnar to prismatic habit, and only one crystal on matrix was tabular with significant differences of thickness between prism faces in different directions.

Idealized crystal drawings are presented in figure 3. Considering the columnar to prismatic crystals and the tabular crystals in our sample set, dominant crystal faces were the first-order hexagonal prism *m* {10$\bar{1}$0} and the basal pinacoid *c* {0001}. These were frequently in combination with a smaller second-order hexagonal prism *a* {11$\bar{2}$0}, and/or first-order hexagonal dipyramids *p* {10$\bar{1}$2} and *u* {10$\bar{1}$1}, and/or a second-order hexagonal dipyramid *s* {11$\bar{2}$2}. In addition, two crystals showed small dihexagonal prism faces *i* {21$\bar{3}$0}, in combination with the second-order hexagonal dipyramid *f* {33$\bar{6}$2} and the dihexagonal dipyramid *k* {21$\bar{3}$1}. The faces determined on conical or at least partly conical crystals were identical to those observed on all other emeralds.

So far, the morphology is consistent with the published literature data above and information determined from photos of Colombian emerald crystals in numerous publications. The two dipyramids *f* and *k* are rarely found in Colombian samples, as previously mentioned by Vrba (1881).

Growth Features on Crystal Faces. Numerous Colombian emerald crystals from the present study showed growth features on crystal faces, especially elongated stepped surface structures on *m* prism faces (figure 4, A and B). These as-grown surface features represent layered growth in subsequent growth steps and resemble contour lines in topographic maps. In sample 1 shown in figure 4, different layers are already seen with the unaided eye, but normally the steps between subsequent layers are smaller and need examination by optical microscopy. To best observe the layered surface structures with optical microscopy, reflected light is ideal (figure 4C). Similar growth layers on the basal pinacoid of the majority of Colombian emeralds, if present, are less pronounced and often not observable at the magnification applied in this study.

These observations are consistent with the existing literature about growth mechanisms of beryl crystals. Similar stepped growth layers of surfaces of beryl crystal faces have been described by various authors (von Kokscharow, 1881; Himmel and Schmidt-Zittel, 1927; Griffin, 1951a,b; Seager, 1953; Grigor'ev, 1965;

Figure 4. A and B: In sample 1 (11.8 mm in length), stepped surface structures on different prismatic m *faces of a Colombian emerald crystal represent layered growth in subsequent growth steps. C: Best observation of such layered stepped growth structures is achieved in reflected light. Photos by G. Martayan (A and B) and K. Schmetzer (C; field of view 6.0 mm).*

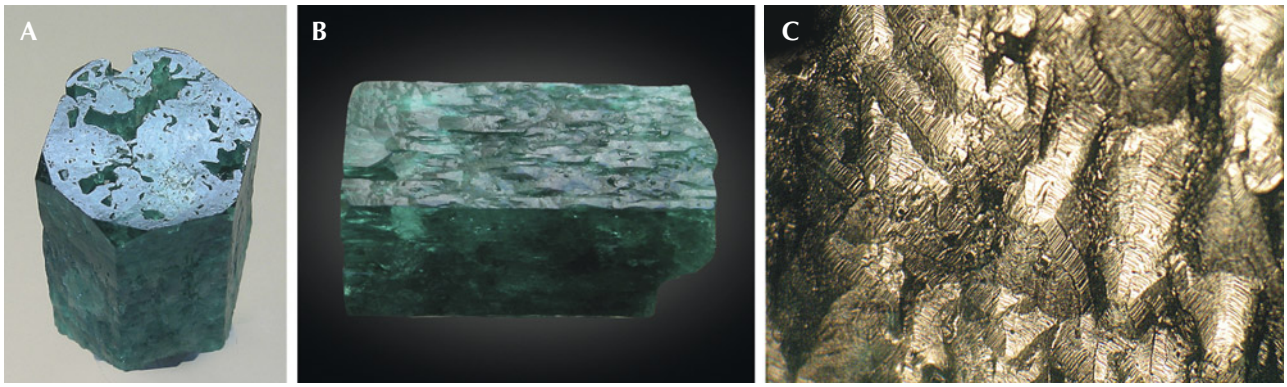

Figure 5. Sample 2 (18.0 mm in length), a columnar emerald that has been heavily corroded by natural etching. A: The basal plane shows irregularly shaped openings to larger cavities below this face. B: The m *prism planes show etch structures, especially irregularly oriented grooves between hillocks. C: Details of the etch structures with grooves and hillocks, seen on the* m *prism face in image B, which are covered by micro-steps as seen in reflected light. Photos by K. Schmetzer; field of view 3.5 mm (C).*

Sinkankas, 1981; Sunagawa and Urano, 1999; Sunagawa, 2003; Demianets et al., 2006).

Characteristics of Individual Groups of Samples with Respect to Growth or Post-Growth Surface Patterns. *Emeralds with Dissolution Features*. A group of three samples with "common" habit (samples 2, 3, and 4) showed pronounced dissolution features with partially dissolved (corroded) crystal surfaces. In the groups describing samples with extraordinary and rare habits in the following sections, some emeralds that have undergone dissolution are also mentioned. To understand the various observations, one general aspect should be mentioned at the beginning of this section: Some of the crystals examined in this study show strong etching and dissolution features only at part of the surface. This indicates that only these parts of the emerald crystals were exposed to the aggressive dissolution fluid and the other parts of the crystals were shielded from the fluid. It can be assumed that such shielding processes were caused by different minerals of the assemblage found in Colombian emerald deposits, which were in close contact with the emeralds' as-grown surfaces (crystal faces). In the present state, these minerals are at least partially dissolved or broken away, now exposing the crystal faces of the emeralds for visual examination.

Sample 2 (figure 5A) with columnar habit (see figure 3B) shows distinct corrosion features. The basal face reveals several irregularly shaped openings to a cavity below this plane, which is larger than the openings, extending widely into the crystal. Prism faces are completely covered by etch structures (figure 5B). Between the deep irregular grooves, small hillocks are observed that show micro-steps on the surface (figure 5C). These micro-steps resemble the pattern produced as fine structure in etch pits by artificial dissolution of beryl crystals (see box A). It is unknown and must be examined in additional samples, which are not available at the moment, whether this pattern and the form of the irregularly shaped grooves are related to the common inclusion features of Colombian emerald (e.g., feathers and healed fractures).

Sample 3 with tabular habit shows a completely and irregularly dissolved surface of the *m* prism, but the smaller *a* prism is not corroded (figure 6A). Only small parts of the original surface of the *m* prism are still present, reflecting under appropriate illumination (figure 6B). In this case, we can speak of a preferred dissolution of the *m* prism compared to the *a* prism face. The basal face shows irregularly terminated openings to deep cavities, but part of this face contains no dissolution features (figure 6C), and therefore it might be concluded that this face was shielded by minerals from the dissolution fluid.

Sample 4 shows long prismatic habit with first- and second-order *m* and *a* prism faces (figure 3A). Toward one end of the crystal, the prism faces show growth steps of an almost undistorted surface (figure 7A). This part represents about one-third of the length of the crystal. The remaining part is extensively etched, deeply corroded on *m* faces and to a much lesser extent on *a* prism faces (figure 7, A and B). In some areas, the *m* prism faces are completely dissolved to an area with numerous grooves and hillocks. In contrast, we observe highly reflective

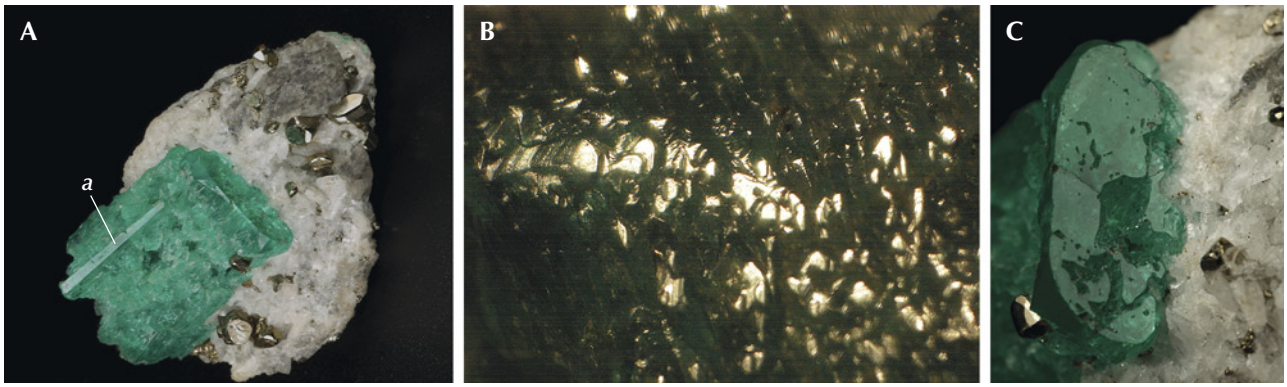

Figure 6. A: Sample 3 (23.6 mm in length), a heavily corroded emerald crystal with a completely dissolved surface related to the m *prism face, but with a small protruding area related to the* a *prism that is almost free of corrosion. B: Only small areas of the original surface of the* m *prism are still reflective. C: The* c *basal pinacoid reveals irregularly shaped holes leading to cavities below this face. Photos by G. Martayan (A and C), and K. Schmetzer (B); field of view 7.6 mm (B).*

ledges of the *a* prism protruding from the dissolved *m* growth sectors (figure 7B). This indicates that, as also observed in sample 3, the *a* prism sectors were less intensely corroded. At the end, one basal pinacoid is only influenced slightly or not at all by corrosion, while the other basal plane on the other end of the crystal is heavily dissolved (figure 7, C and D).

Evaluation. Comparing these observations with descriptions from the known literature (box A), it is concluded that samples 2–4 have undergone a heavy natural dissolution process in which the original surfaces of the crystal faces were partially or completely dissolved by natural etching. In other words, the patterns observed in our Colombian samples are related to intense natural etching processes causing at least a partial dissolution of the as-grown crystal faces and creating deep cavities and irregular grooves between hillocks with stepped surfaces. All three crystals show

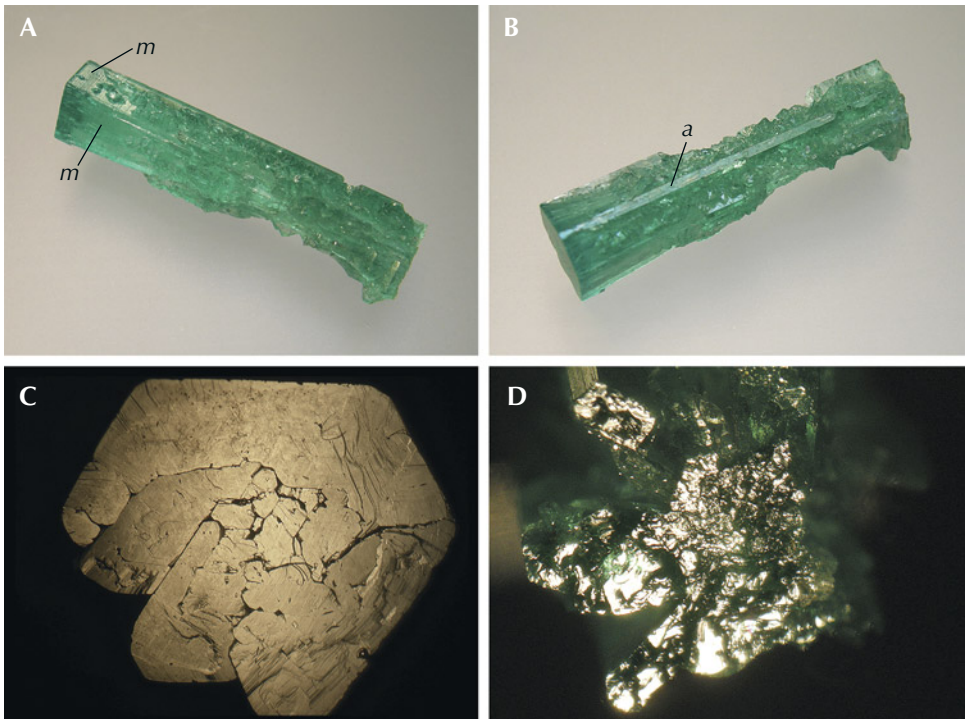

Figure 7. Sample 4 (31.1 mm in length), a columnar emerald that has been heavily corroded by natural etching. One end of the crystal (A, upper left) still shows natural crystal faces, while the rest of the sample shows completely dissolved m *prism faces (A and B) and highly reflective but still undissolved smaller* a *prisms (B). At one end, the basal face is only slightly corroded (C), while the basal face at the other end of the crystal is heavily corroded (D). Photos by K. Schmetzer; field of view 9.5 mm (C and D).*

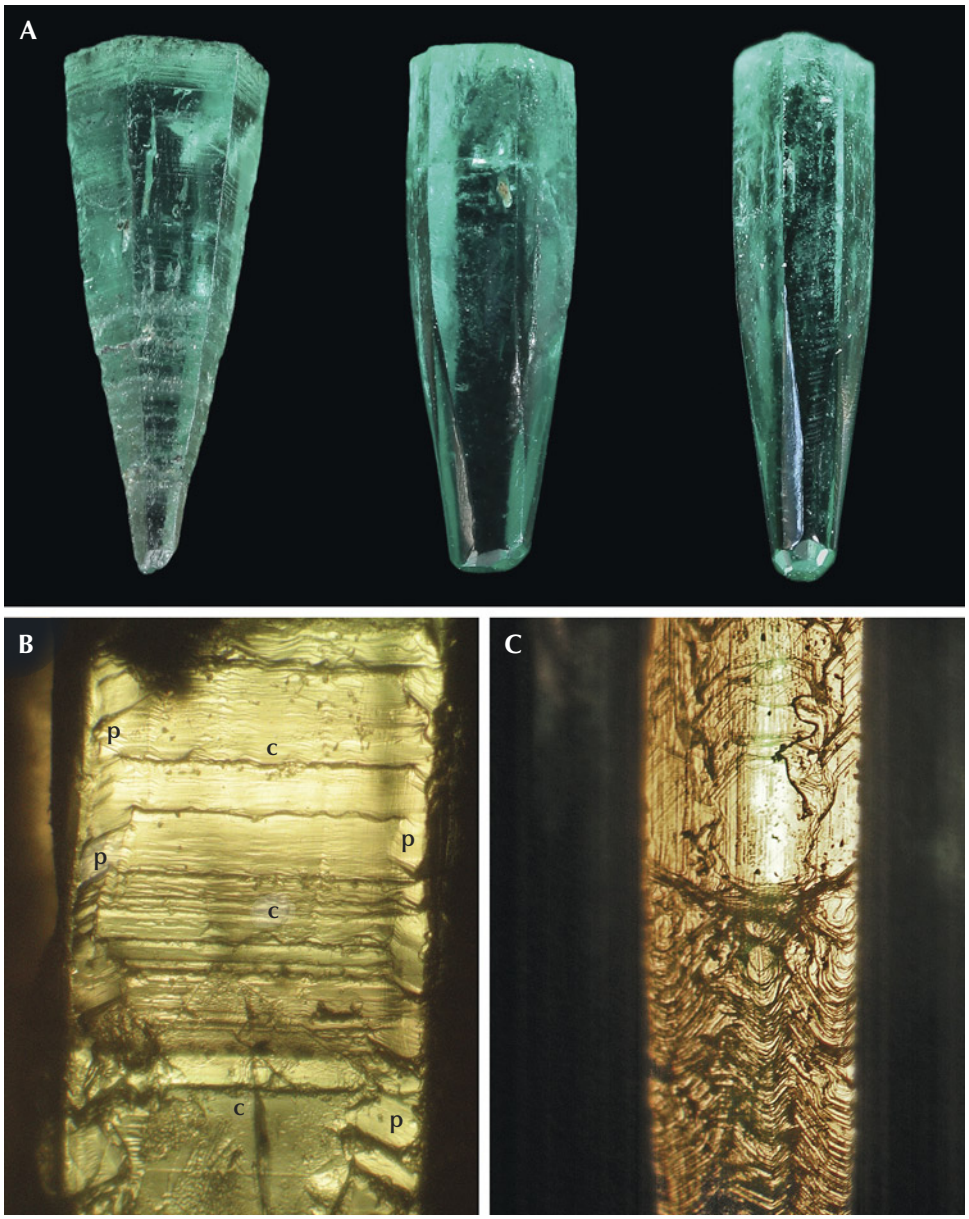

Figure 8. A: Emerald crystals with pyramidal or partly pyramidal habit: sample 5 (left, 10.0 mm in length), sample 7 (center, 8.8 mm in length), and sample 6 (right, 8.8 mm in length). B: Surface texture of the pyramidal emerald crystal (sample 5) showing growth lines related to the basal pinacoid c *(center) and pyramidal faces* p *(left and right). C: Complex surface texture of a partly pyramidal, partly prismatic crystal (sample 7) showing a complex pattern related to pyramidal faces (lower part) and to basal, pyramidal, and prism faces (upper part). The growth direction of the crystals shown in A–C is always from the bottom to the top. Photos by G. Martayan (A) and K. Schmetzer (B and C); fields of view 2.4 mm (B) and 2.4 mm (C).*

various dissolution features on different surfaces. Sample 4, for example, shows heavy dissolution from one end with a dissolved basal *c* face to almost two-thirds of its length, while the other end with basal *c* face to about one-third of its length is barely affected. In samples 2 and 3, it seems that the basal *c* faces were partially shielded from the dissolution fluid.

An emerald with pointed forms (sample 10) caused by natural etching will be described in the next section.

Emerald Crystals with Conical Habit or Conical Zones. Several samples showed, at least partly, a conical habit, comparable to six-sided pyramids.

Referring to the observations made in this study for samples 5–10, the authors must underscore that with the optical methods applied, we only can describe the features representing the last stage of growth and/or dissolution.

Three relatively small emerald crystals, designated samples 5, 6, and 7, show the habit of a six-sided pyramid or the habit of a six-sided pyramid combined with a six-sided prism (figure 8A). The surface texture of the pyramidal sample 5 shows growth steps related to basal and pyramidal growth layers (figure 8B). The basal growth layers are visible as striations perpendicular to the *c*-axis, which indicate alternating basal and dipyramidal faces. The surface

texture of samples 6 and 7 is more complex. In the pyramidal parts, growth steps related to basal and pyramidal layers are seen; in the prismatic parts, the crystals show textures related to basal, dipyramidal, and prism faces (figure 8C). These observations were confirmed in immersion with transmitted light (not shown). In the conical parts of all three samples, no growth layers related to prism faces were developed. In contrast, the prismatic parts of samples 6 and 7 are quite "normal," with growth zones related to basal, pyramidal, and prismatic faces.

Sample 8 consists of a conical and a tabular part (figure 9). At the upper (conical) end of the crystal, we observe a perfect basal face in combination with part of the *m* prism faces and *s* and *p* dipyramids (see figure 3C). Next to this end of the crystal, we observe a conical part, followed by a tabular area. The diameter of this tabular area is slightly larger than the crystal's diameter at the upper end. Growth steps are found on the surfaces of the conical area (figure 9C) and on the tabular part. Only the outer area of the tabular part contains growth channels (hollow tubes) parallel to the *c*-axis. In transparent areas of the conical part, internal growth planes parallel to the basal pinacoid *c* and parallel to two hexagonal dipyramids *p* and *u* are observed in immersion (figure 9D). These features indicate growth in subsequent layers, but without development of prismatic growth sectors in this area of the crystal.

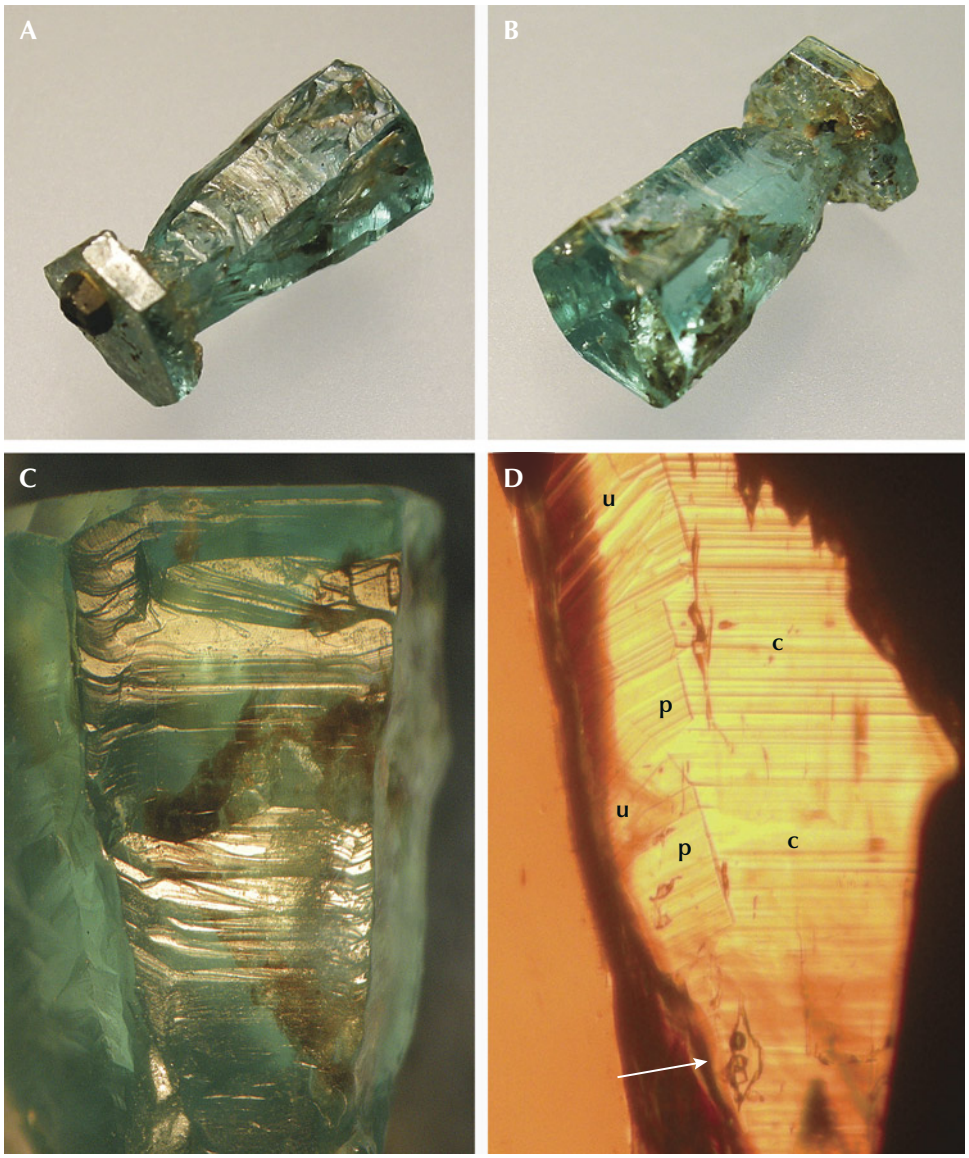

Figure 9. A and B: Sample 8 (9.8 mm in length), an emerald crystal with conical shape and a tabular part, with a pyrite crystal attached to the tabular part. C: Growth steps on the surface of the conical part of the crystal. D: Viewed in immersion, internal growth planes parallel to the basal face c *and parallel to the hexagonal dipyramids* p *and* u*, as well as a three-phase inclusion with two salt cubes and one gas bubble in a liquid-filled cavity (arrow); the* c*-axis runs vertically. Photos by K. Schmetzer; fields of view 5.7 mm (C) and 2.2 mm (D).*

Sample 9 is of conical shape. At the upper (wide) end of the crystal, we observe a perfect basal face in combination with part of the *m* prism faces and *s* and *p* dipyramids (figures 3C and 10A). The *m* prism faces reveal growth steps (figure 10B), while the conical part is covered with finer surface structures. We observe irregularly shaped grooves, hillocks covered by micro-steps, and openings of deep cavities or indentations (figure 10C). Comparing these surface textures with those of corroded emerald samples 2, 3, and 4, these parts of sample 9 were exposed to an aggressive fluid causing dissolution. Within some of the indentations mentioned, residual dark gray carbonaceous material is captured (figure 10D).

Sample 10 shows an even more complex morphology. The crystal consists of a conical part that is followed by a prismatic part at the lower end of the crystal (figures 1 and 11A). The prismatic part is narrower than the conical part at its upper end. The surfaces on both parts show growth steps (figure 11, B and C). Protruding from both parts are two areas with extensions of growth sectors confined by the second-order hexagonal prism *a*, which are as thick as the upper end of the conical part (figure 11A). The basal pinacoid is covered by tiny pointed hillocks (figures 1 and 11D). By varying the crystal's orientation with respect to the light source, positions can be found where multiple small crystal faces covering different hillocks reflect light simultaneously (figure 11D).

Evaluation. The growth history of natural beryl crystals frequently shows multiple subsequent growth steps that might be separated by partial dissolution from natural corrosion and etching. The different steps of growth history of such samples have been characterized by a combination of optical and X-ray topography methods, especially for oriented slices of the original crystals (Scandale et al., 1990; Sunagawa and Urano, 1999; Sunagawa, 2003).

In our study, all samples of this group show one common morphological feature: a tapered appearance, at least in parts of the crystal. This feature is caused by a growth process in which no prismatic growth sectors were developed during crystal growth. This indicates that the conical appearance is caused by basal and pyramidal sectors growing together, which are seen on the surface of the crystals in reflected light or in immersion in transmitted light. In the conically developed sample 5, we observe only such basal and pyramidal growth layers. Samples 6 and 7, in addition to a conical part, developed prismatic parts in later growth stages (see again figure 8).

Samples 8, 9, and 10 are emerald crystals with an even more complex growth history. In all three samples we observe growth stages in which basal and

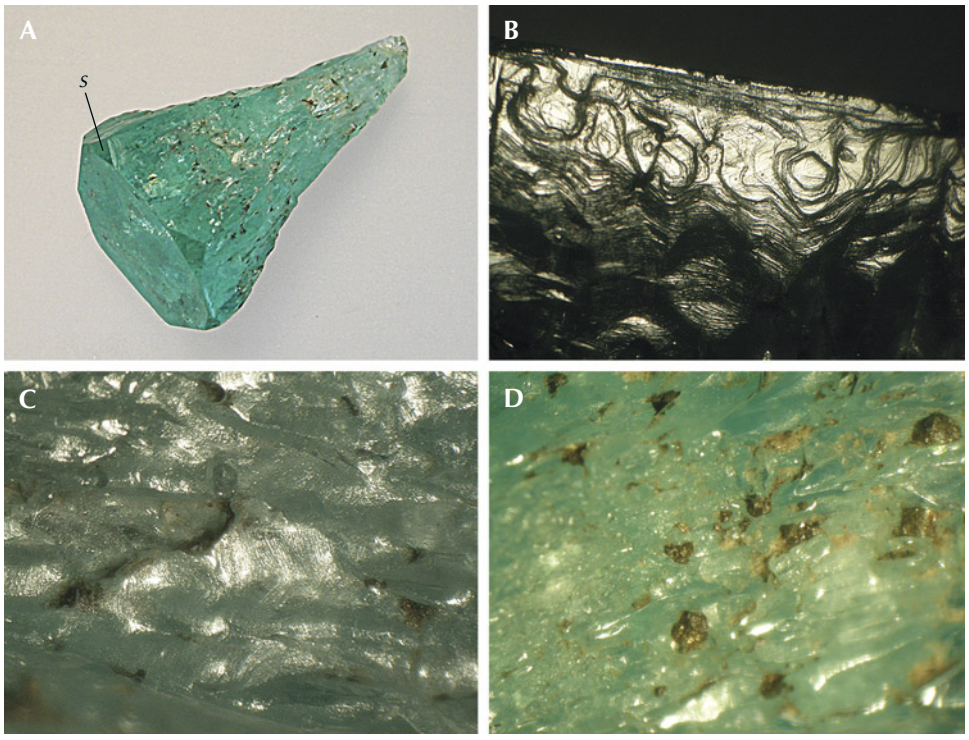

Figure 10. A: Sample 9 (20.8 mm in length), an emerald crystal with conical shape, with basal pinacoid c*, small* m *prism faces, and hexagonal* s *dipyramids. B: Growth steps on the surface of one of the* m *prism faces, viewed almost perpendicular to the* c*-axis. C: Hillocks with fine microsteps between irregularly shaped groves on the surface of the conical part. D: Residual dark gray carbonaceous material captured in indentations on the surface of the conical part. Photos by K. Schmetzer; fields of view 4.5 mm (B), 3.5 mm (C), and 7.6 mm (D).*

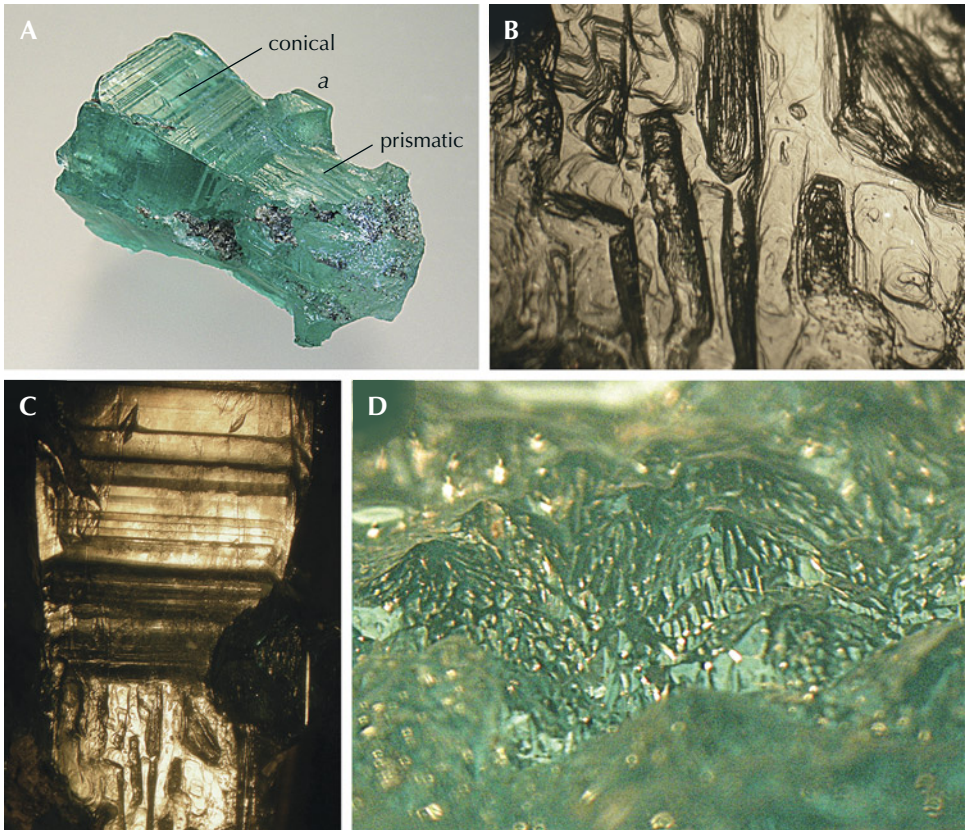

Figure 11. A: Sample 10 (25.0 mm in length), an emerald with conical habit in the upper left and prismatic habit in the lower right; the base is covered with numerous hillocks; a protrusion at the conical part represents a growth sector confined to the prism a. *B: Stepped surface texture of the prismatic part. C: Growth steps at the prismatic part (bottom) and the conical part (top), and the* c*-axis runs vertically. D: On the basal face, the surfaces of the hillocks consist of numerous small faces that reflect light; viewed oblique to the* c*-axis. Photos by K. Schmetzer; fields of view 5.7 mm (B), 9.5 mm (C), and 5.0 mm (D).*

dipyramidal growth sectors were developed, but without development of related prismatic growth layers. These growth stages without formation of prismatic growth layers apply at least to part of the crystal's growth history.

In the tabular area of sample 8, we observe growth channels parallel to the *c*-axis, which were not seen in the tapered part of the crystal. The diameter of the tabular area is larger than the diameter of the conical part at its upper end. This might indicate a later partial overgrowth of a crystal with conical habit and, in this later growth period, the development of a tabular area, on top of the tapered part of the crystal (see again figure 9).

Sample 9, at its wider end, has a short prismatic area and a long, tapered cone. This cone shows dissolution features on its surface. These features indicate an etching process of the conical part after crystal growth and a subsequent growth step with the formation of prismatic layers at the end of the crystal (see again figure 10).

Sample 10 has likely undergone several growth and corrosion processes. The residual parts of prismatic *a* growth zones and the small pyramids or hillocks forming the end of the conical part of the crystal indicate strong corrosion after an initial growth step (see references cited above). Skeletal growth (see box B and examples below) with pointed pyramids and sharp hillocks has never been mentioned in any beryl and is therefore considered very unlikely for this morphological structure.

After corrosion, we observe several subsequent growth steps, in which an area with prismatic growth layers and the conical zone with basal striations were developed. Obviously, in one of these growth steps, only basal growth layers without prismatic areas were formed. It is not completely understood whether the prismatic *m* growth sectors in the lower part of the crystal were grown before or after the conical zone with tapered surface of the crystal (see again figure 11).

Emeralds with Incomplete Growth of the Basal Face. Several variants of incomplete growth of the basal pinacoid were observed.

Samples 11, 12, and 13 show incomplete growth of the basal face *c*, a pattern that could be described as resembling surface indentations. Sample 11 (figure 12A) is a single emerald crystal on matrix and reveals well-developed prism and pyramidal faces. Sample 12 (figure 12B) is an aggregate of approximately 11 crystals, grown parallel to each other with somewhat different lengths. All crystals of this aggregate show

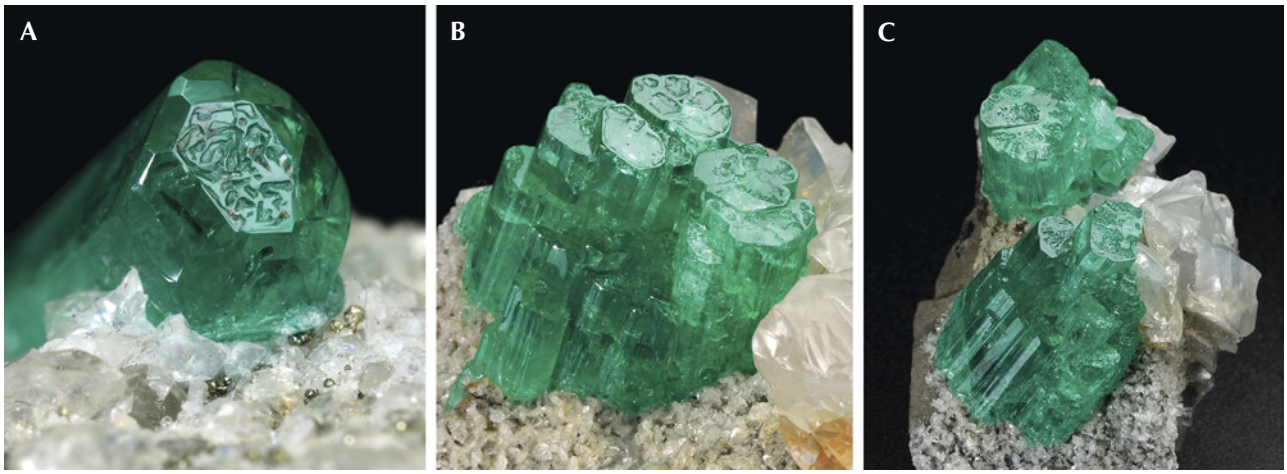

Figure 12. Emeralds with surface indentations on the basal face, developed as either a single crystal (A: sample 11, 4.1 mm in largest diameter) or as aggregates of parallel emerald crystals (B and C: samples 12 and 13 with crystal length up to 12.5 mm and 16.5 mm, respectively). Photos by G. Martayan.

incompletely developed *c* faces. Sample 13 (figure 12C) is similar to sample 12, but with three such aggregates consisting of approximately nine, eight, and three emerald crystals. All basal faces have a stepped micro-texture consisting of numerous layers stacked parallel to the *c*-axis of the emerald crystal (figure 13, A–C). These structures occasionally end at the level of the horizontal surface of the rim, but some columns or other structures have different heights within the rim. In addition, all three samples have a step-like texture on prism faces and no etch features. A representative example of that pattern is shown in figure 13D.

Samples 14 and 15 show somewhat deeper indentations on the basal faces. Sample 14 has an almost continuous rim parallel to the basal face and inside several hillocks within the indentation zone (figure

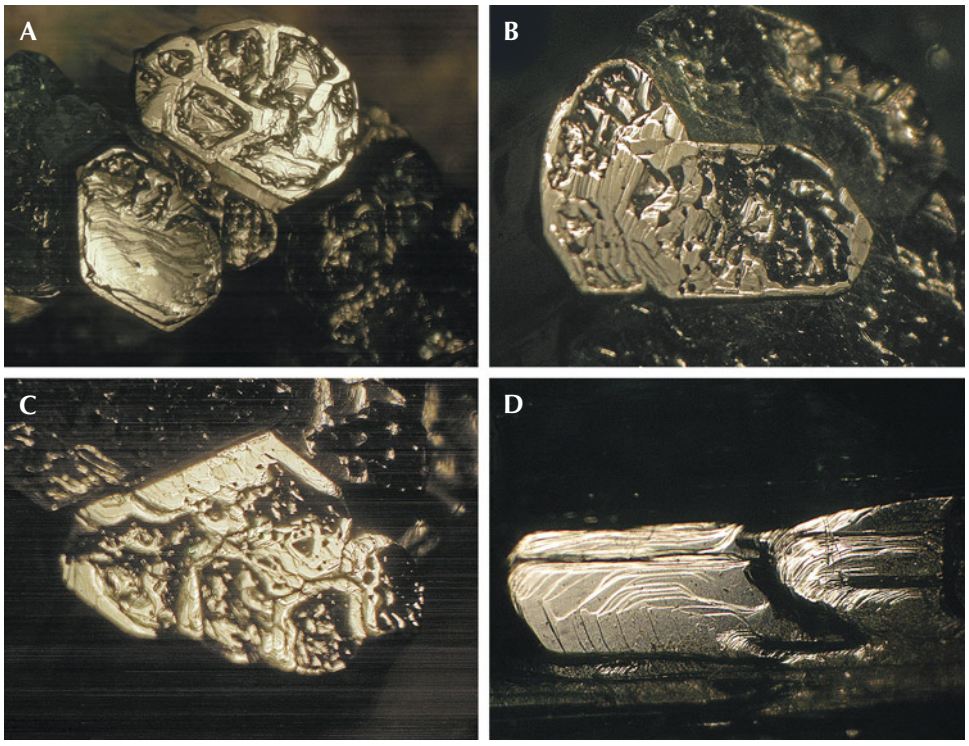

Figure 13. A–C: The stepped micro-texture of emeralds with incompletely developed basal planes shows stacked layers parallel to the c*-axis. D: Growth steps on the* m *prism face of one of the crystals in figure 12B. Shown here are sample 12 (A and D) and sample 13 (B and C). Photos by K. Schmetzer; fields of view 11.5 mm (A), 7.6 mm (B and C), and 4.6 mm (D).*

Figure 14. Left: Sample 14 (6.0 mm in largest diameter), a crystal with an almost continuous rim surrounding growth areas ending in small basal faces, but at a different height along the c*-axis compared to the horizontal surface of the rim. Right: Reflective areas of the rim and the small columns inside this rim ending in tiny crystal faces parallel to the basal pinacoid. Photos by G. Martayan (left) and K. Schmetzer (right).*

14, left). Part of these hillocks in the form of tiny columns end with faces parallel to the base (figure 14, right), but lower than the horizontal surface of the rim, which is formed by the incomplete basal face of the crystal. Sample 15, with similar appearance, shows an almost colorless region that ends in a basal face with indentations (figure 15A). The end of the crystal with these indentations is separated from the main part by a small zone with intense green coloration (figure 15B). This demonstrates that at the beginning of the growth of this zone with a length of about 1.5 mm along the *c*-axis, growth conditions were different compared to the earlier growth stages. Hollow channels parallel to the *c*-axis are found in all parts of the crystal. The areas parallel to the basal face show growth steps (figure 15C).

Several crystals were formed as "emerald cups." Sample 16 is a crystal with columnar habit in the form of an open cup. The morphology consists of first- and second-order prism faces in combination with first- and second-order hexagonal dipyramids (figure 3C and figure 16, A and B). The *m* prism faces are planar; no growth steps or etch features were visible in the optical microscope with the magnification applied. The wall thickness of the cup varies between 0.8 and 1.4 mm. Irregularly shaped hillocks or columns cover the bottom of the cup, which forms a clear boundary with the other part of the crystal (figure 16C). In a view parallel to the *c*-axis, a microstructure is observed forming a three-dimensional framework of walls, columns, and hillocks at the bottom of the cavity (figure 16D). Part of the columns or irregular walls end in planar faces parallel to the basal pinacoid (figure 16, A and B).

Sample 17 is a piece of black shale covered by albite, calcite, and pyrite crystals. Embedded in this matrix are five emerald crystals (figures 2 and 17A). Two of these are columnar and hollow, forming deep

Figure 15. A: Sample 15 (37.4 mm in length), an emerald crystal with color zoning; at one end, the sample reveals a continuous rim surrounding growth areas ending in small basal faces. B: Growth and color zoning (arrows) of the crystal along the c*-axis. C: Areas of the rim and small columns inside the rim with planes parallel to the basal pinacoid appear bright in reflected light, viewed parallel to the* c*-axis. Photos by K. Schmetzer; field of view 3.6 mm (C).*

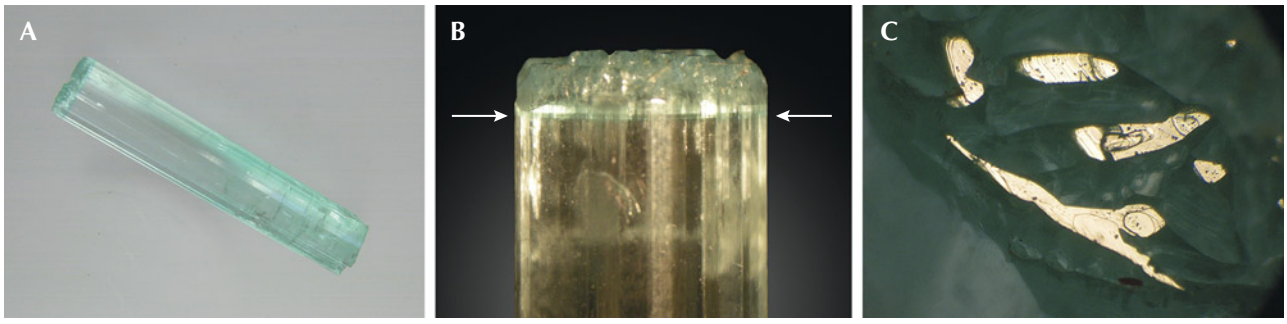

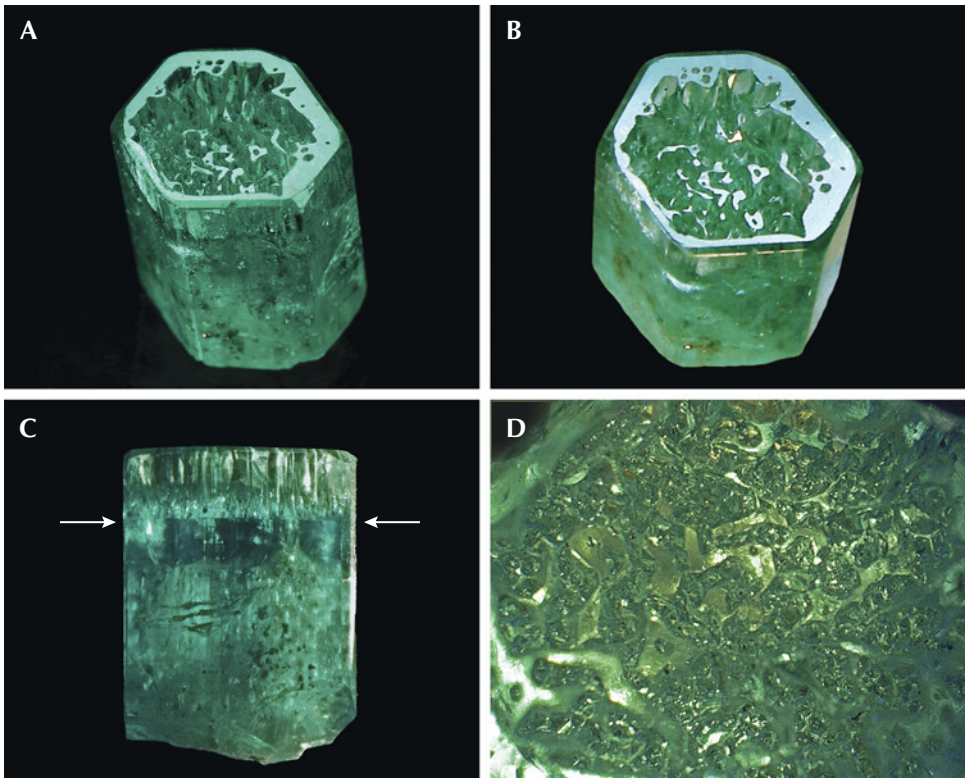

Figure 16. A: Sample 16 (10.8 mm in length), an emerald crystal developed in the form of a cup. B: The basal plane of the cup reflects together with the basal faces of small hillocks or columns in the cup. C: The bottom of the cup is located in the upper half of the crystal, as indicated by arrows. D: Framework of irregular hillocks, columns, and walls on the bottom of the cup in a view parallel to the c*-axis. Photos by G. Martayan (A) and K. Schmetzer (B–D); field of view 4.6 mm (D).*

cups with one open end (figure 17B). The cups have a wall thickness of approximately 0.5 mm. The bottom of each cup is covered with emerald hillocks or columns, which frequently end within the hollow space of the cups with irregularly shaped planes. Other planes at the ends of the tiny crystals in the hollow cups reflect together with the residual basal face of the rims (figure 17C), indicating that some of

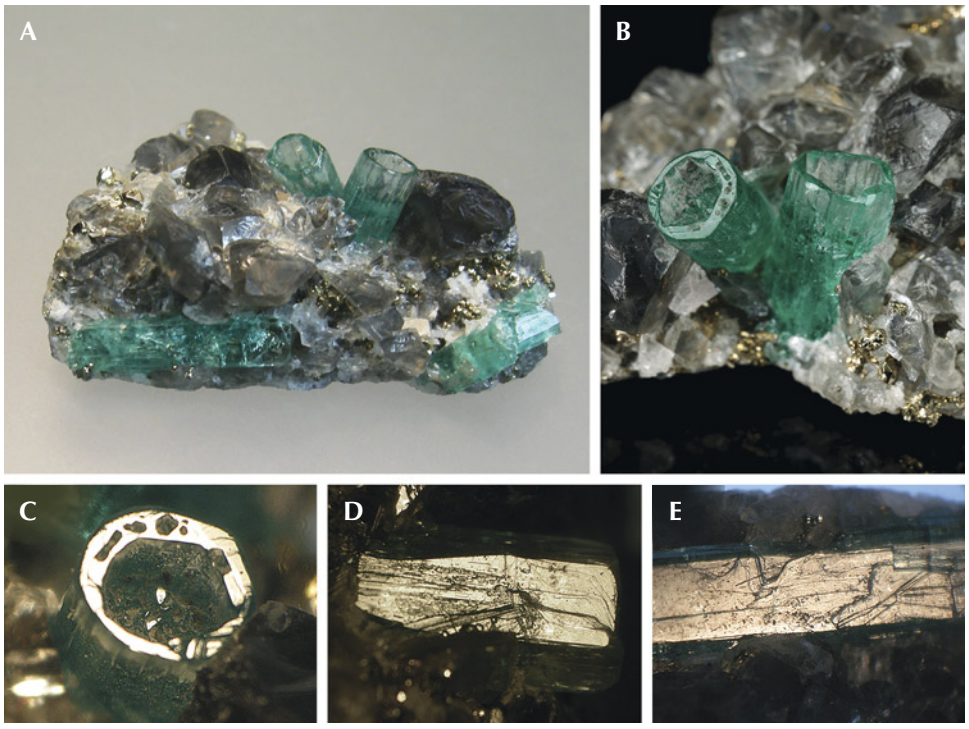

Figure 17. A: In sample 17 (26 mm long), a base of black shale (not visible) is covered with albite, calcite, and pyrite crystals. In this matrix, five emerald crystals are embedded, two of them as deep cups (center) and three as "normal" emeralds (lower right and left). B: Details of the two emerald cups (5.5 mm long on the right). C: In reflected light, the basal plane of one cup appears bright together with the basal faces of small hillocks or columns in the cup. D: Growth steps on the surface of one m *prism face of a cup. E: Growth steps on the surface of the* m *prism face of a "normal" emerald crystal. Photos by K. Schmetzer (A, C–E) and G. Martayan (B); field of view 7.6 mm (C–E).*

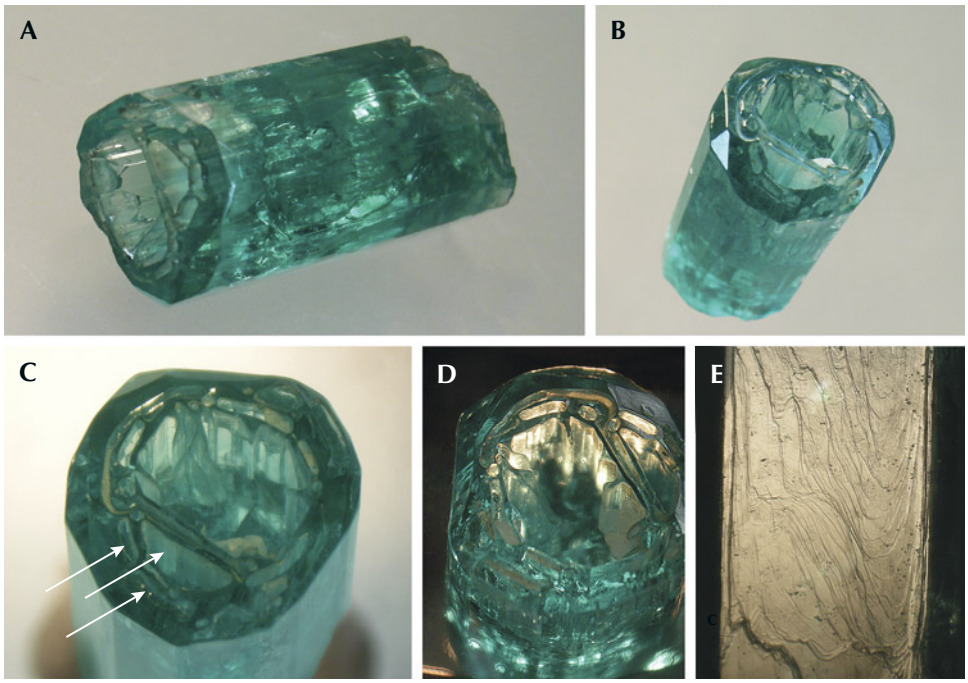

Figure 18. A and B: Sample 18 (19.6 mm in length), an emerald crystal developed in the form of a deep cup. B and C: Openings at one end are developed in the basal pinacoid but also in the largest p *dipyramid (arrows); within the cup, a framework of irregularly shaped thin emerald walls is present. D: The crystal faces at the inner surface of the wall are oriented parallel to the outer prism faces. E: Growth steps on the surface of an* m *prism. Photos by K. Schmetzer; fields of view 11.5 mm (D, vertical) and 5.1 mm (E).*

the hillocks or columns also end in faces parallel to the basal pinacoid. The *m* prism faces of the cups show growth steps (figure 17D).

The three other emerald crystals are "common" columnar crystals with prismatic and basal faces (figure 17A), which also show growth steps on *m* prism faces and no etch features (figure 17E).

Sample 18 is the largest crystal, in the form of a deep open cup (figure 18, A and B). Morphologically, the columnar and somewhat distorted crystal shows several prism faces and hexagonal dipyramids (see figure 3, C and D). The main opening at one end is in the basal pinacoid, but holes are also developed in the largest *p* dipyramid (figure 18C). The cup's wall thickness ranges from 1.5 to 2.0 mm. Within the cup, a framework of irregularly shaped thin emerald walls is present (figure 18, B and C). The main walls of the inner surface of the rim are oriented parallel to prism faces (figure 18D). The outer *m* prism faces are covered by growth steps (figure 18E).

Sample 19 is considered to be a half cup. Formally, the sample is described as a crystal formed of two parts. The first part shows platy habit, with two basal *c* faces and *m*, *a*, and *i* prism faces (figure 19A). On

Figure 19. A: Sample 19 (7.8 mm in length), an emerald crystal in the form of a half cup developed with two parts: as a platy part with lower and upper basal pinacoid (white arrows) and an upper curved rim surrounding about half of the area of the platy part; this rim is terminated by a small basal face (red arrow). B: Stepped surface of the basal face on top of the horizontal surface of the rim. C: View of the inner surface of the circular rim on top of the platy part, in this orientation with reflective steep k *hexagonal dipyramids, the elongated cavities are filled with fine-grained white beryl. Photos by G. Martayan (A) and K. Schmetzer (B and C); field of view 14.5 mm (B).*

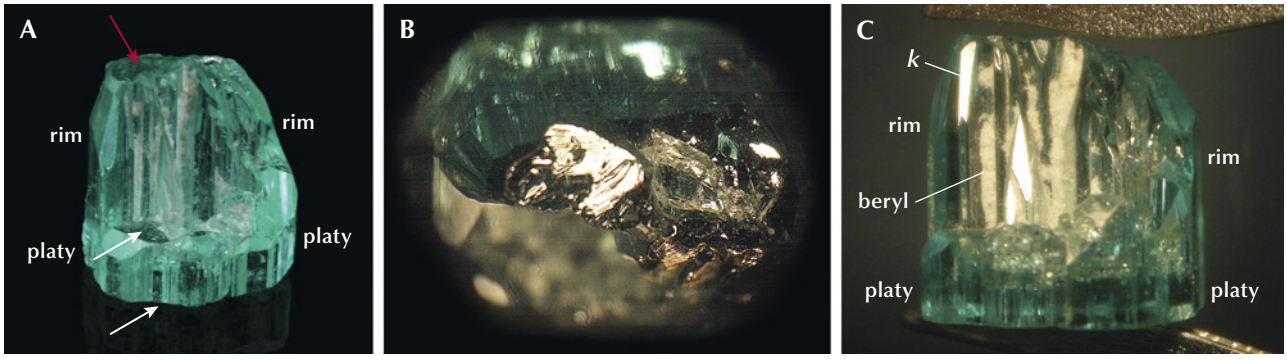

the upper side of the first part of the crystal, a curved rim is formed that encircles about half of the area formed by the prism faces of the first part. This rim is considered to be the second part of the crystal. On top of this rim, we observe a small area with a stepped surface in an orientation parallel to the basal pinacoid (figure 19B). We can consider this to be the end of the second part of the crystal.

The other faces of the outer surface of the rim are the already mentioned prism faces *m*, *a*, and *i* in combination with *u*, *p*, *s*, *f*, and *k* dipyramids. Not only are the *f* and *k* dipyramidal faces rarely observed in Colombian emerald, but they are also rarely observed in the mineral beryl as a whole. These faces are steeper than the commonly observed *u*, *p*, and *s* dipyramids and are inclined 18.2° and 18.5° to the *c*-axis. The open structure of the rim allows us to determine the faces at the inner surface of this rim, which are the common prism faces in combination with the two steep dipyramids *f* and *k* (figure 19C). The open cavities formed at the inner surface of this rim, elongated parallel to the *c*-axis, are partially filled with a white fine-grained material, which was determined to consist mainly of beryl with small admixtures of quartz and albite (identified by a combination of X-ray diffraction, EDXRF, and Raman spectroscopy).

Samples 20 and 21 are also incomplete cups with only partially developed walls or rims. In both samples, the bottom of the internal cavity is filled with pyrite crystals, surrounded by an incomplete circle of walls (figure 20). In sample 20, the outer *m* prism faces show growth striations parallel to the *c*-axis, and the internal surface of the walls displays open channel structures, comparable to the open channels observed in sample 19. The outer and inner surfaces of the rim in sample 21 are completely flat.

Emerald Crystal with an Internal Channel. Sample 22 is an elongated tube that is open at both ends. From top to bottom, the external form of the tube is slightly conical, and the channel inside it is also wider at one end, following the external form of the tube (figure 21). The tube was cut at the thinner bottom of the sample, showing a hole with a small diameter (figure 21, left). This indicates that the original crystal might have been closed at its end. At the other end with the larger opening, the thickness of the tube walls ranges from about 0.2 to 0.6 mm, with an opening between 2.5 and

Figure 20. Emerald crystals in the form of incomplete cups with pyrite crystals at the bottom of the cavities, which are surrounded by incomplete rims. Sample 20 on the left is 13.0 mm in length, and sample 21 on the right is 9.0 mm in length. Photos by G. Martayan.

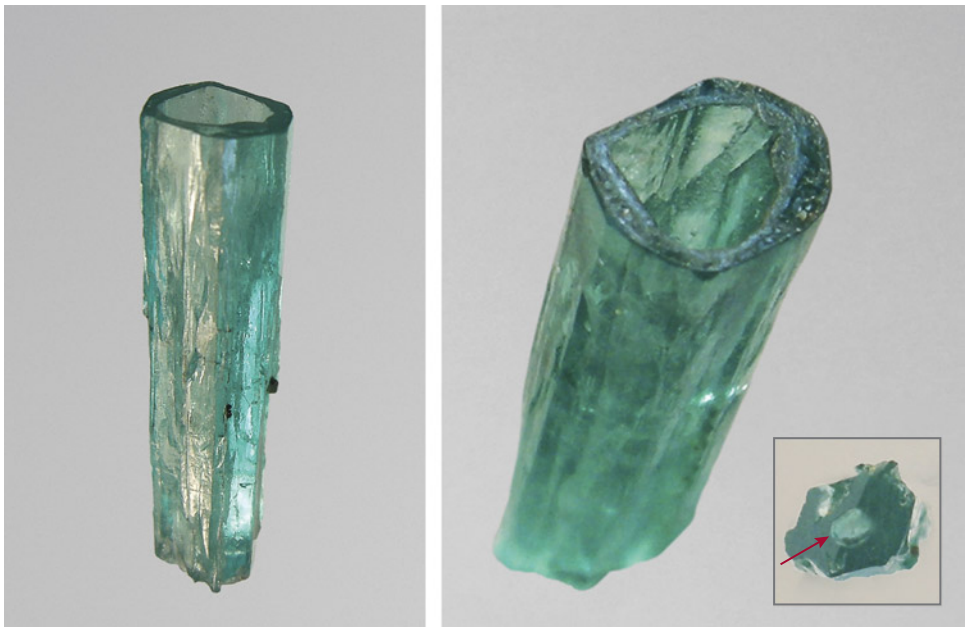

Figure 21. Emerald crystal (sample 22, 14.4 mm in length) in the form of a slightly conical hollow tube (left), with openings at both ends (right). The lower end of the crystal (right, inset) was cut artificially and shows a hole (arrow). Photos by K. Schmetzer.

3.5 mm in diameter. The diameter of the channel through the crystal at the other end is approximately 1.0 mm. Outside, the tube is terminated by *m* prism faces, which show etch features—i.e., the original surface of the tube is partially dissolved (figure 22). The horizontal part of the wall or rim oriented parallel to the basal pinacoid (see figure 21B) reveals small pits, most likely due to etching.

Evaluation. Samples 11–21, all originating from Chivor, show the same phenomenon: incomplete growth of the basal face, but with a different degree of development. In general, our Colombian samples display an upper rim surrounding indentations (see again figures 12 and 13) and somewhat deeper depressions (figures 14 and 15) or somewhat higher walls or rims surrounding deeper cavities (figures 16–20). In other words: The patterns observed in cups of various depths in samples 16–21 or in emeralds with deeper indentations of basal faces in samples 14 and 15 reflect deeper indentation patterns on basal planes than those observed in samples 11–13.

The rims or walls end with faces oriented perpendicular to the *c*-axis, and the outer surface of the rims are formed by various prismatic and pyramidal faces. The inner surface of the walls or rims are formed by the same faces, mainly first- and second-order prism faces and occasionally in combination with steep dipyramids. This means that the outer and the inner outlines of the skeletal beryl walls are parallel to prismatic and steep dipyramidal faces. Within these depressions or cavities, we observe irregular walls or columns, which end at different heights in the cavities with small basal faces. In samples 15 and 16, it is clearly indicated that the inner bottom of the cavities is confined to a zone of strong color zoning, which indicates a change of growth conditions at this stage of crystal growth (see again figures 15 and 16).

Considering the patterns described for beryl with skeletal and polygonal growth (box B), we conclude that the morphology seen in Colombian emerald samples 11–19 can be understood as a combination

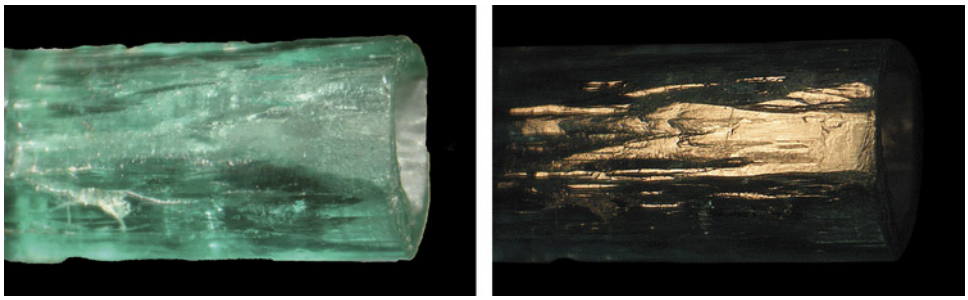

Figure 22. The surface of sample 22 is partially dissolved by corrosion—i.e., no clear reflective plane is seen. The same area of the crystal is shown in transmitted light (left) and in reflected light (right). Photos by K. Schmetzer; field of view 9.5 mm.

of both growth phenomena: skeletal growth of the walls and polygonal growth of columns and walls inside the cavities. Or we could describe the pattern observed as the growth of a dominant wall and the growth of small columns or pyramids within the area surrounded by the rim. Samples 20 and 21 clearly show inhibited growth of emerald (skeletal growth) due to pyrite obstacles, forming cavities with incomplete walls.

Sample 22, the elongated emerald tube, also originates from Chivor. Considering samples 11–21 and the heavily corroded samples 2–4, our understanding of etch patterns in beryl (summarized in box A), and our knowledge about the surface structure of non-corroded emerald crystals (sample 1, figure 4, and other examples in this paper), we interpret the growth history of this sample as skeletal growth followed by etching and partial dissolution of the outer and inner faces of the crystal, i.e. the outer and inner surfaces of the walls, but with no regrowth after etching.

Pignatelli et al. (2022) explained the growth of several Colombian emeralds developed as cups with conical or prismatic shape simply as etching processes, without taking skeletal growth into consideration. While we take into consideration a combination of skeletal growth and post-growth etching for one sample (see description and growth evaluation of sample 22), we cannot support the idea that all growth structures and morphological patterns of samples 11–22 are due to "simple" etching processes. We conclude that, for samples 11–21, they are not even partly related to etching processes.

To support our conclusions with further arguments, we observed several growth features in this group of samples that are not consistent with the idea of etching, starting at an as-grown basal plane. In other words:

- Etching would not create internal prism faces, which form the dominant pattern of inner surface of the circular rims.
- Etching would not stop and form the bottom of cavities just at the height of a strong color zoning along the *c*-axis of the crystals.
- Etching would form stepped surfaces and cavities, but in our samples we observe instead the presence of small basal faces at the end of pyramids or columns of different height within the cavities.
- The layered appearance of the surface of the rim and the *m* prism faces of the crystals does not reflect etching structures.

All these features indicate that the described morphology of this group of crystals cannot be explained simply by etching processes of the basal face. It cannot be assumed that the different morphological forms described are due to etching, starting at one planar basal face and leaving the rest of the crystal, especially all prism faces, without any clear sign of etching.

Comparison with Properties Observed in Cut Stones. It has already been mentioned in various studies that the heavily included areas between the transparent basal and prismatic growth sectors of Colombian trapiche emerald are intensely corroded (e.g., Bernauer, 1926; Nassau and Jackson, 1970; Pignatelli et al., 2015). In general, Colombian trapiche emeralds consist of a basal growth sector in the form of a tapered core and six prismatic growth sectors. The core and the six prismatic growth sectors and each of the prismatic sectors are separated from others by areas with high concentration of mineral inclusions and carbonaceous material. The basal growth sector mainly consists of basal and occasionally of pyramidal growth layers, but without any prismatic growth areas.

Corrosion, in general, commences at crystal defects that could be lattice defects or areas at trapped inclusions. Sample 9 described here might represent the final stage of such corrosion processes. The general appearance is reminiscent of the central tapered core of trapiche emerald (figure 23). Furthermore, we observed etch structures and residual dark gray carbonaceous material. This indicates that the tapered sample examined in this paper might be the core of a trapiche emerald that was separated from its prismatic growth zones by etching processes. If this interpretation is correct, the prismatic growth layers at the upper end of the crystal (see figure 10B) might be understood as later overgrowth of the tapered crystal.

The irregularly shaped hillocks, columns, or walls within the cavities of the samples with surface indentations on basal faces—i.e., the emerald cups described in samples 11–19—resemble the internal growth structure found in the so-called *gota de aceite* emeralds (figure 24; e.g., Bosshart, 1991; Ringsrud, 2008; Hainschwang, 2008; Schmetzer, 2009; Gao et al., 2017). An overgrowth of the polygonal patterns within such a crystal, especially in crystals with shallower indentations as seen in samples 11–13 (figures 12 and 13), in further growth steps would result in emerald crystals with the characteristic *gota de aceite* structural inclusion pattern. It is plausible

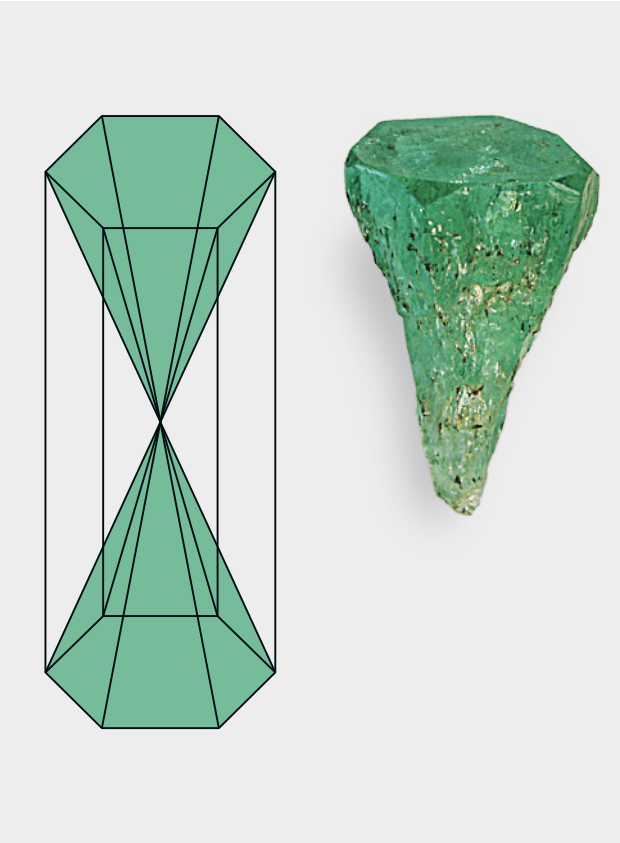

Figure 23. Left: Diagram of a trapiche emerald consisting of two tapered cores representing basal growth sectors (green) and six prismatic growth sectors (after Schmetzer, 2019). Right: The outline of sample 9 conforms to the shape of one of the basal growth sectors in trapiche emerald.

that, with changing environmental growth conditions, such further growth steps could take place. A general scenario with a multistep growth history has already been proposed by various authors (e.g., Gübelin and Koivula, 2008; Ringsrud, 2009; Schwarz and Curti, 2020; Sun and Goa, 2022).

SUMMARY AND CONCLUSIONS

Most Colombian emeralds show a columnar to prismatic habit with growth steps or growth layers on prism faces, which can be seen occasionally even with the unaided eye. Several groups of samples with specific morphological patterns on the surface have been studied and described. However, some of the samples from our study theoretically could be grouped into several different categories, simply because they have undergone several subsequent growth stages and dissolution processes (e.g., sample 10). Because optical observation allows us to examine only the last result of such multistep growth processes, not all morphological features of the emerald crystals in the post-grown and post-dissolved state can be completely understood.

Heavily etched crystals show dissolved *m* prism sectors, whereas the *a* prism zones are less affected by the dissolution process. The deep cavities or grooves seen in the post-growth dissolved state have a stepped microstructure on *m* prism faces. The basal pinacoid, in some cases, reveals irregularly shaped openings to cavities below that face, but this face may also be dissolved in a way to show tiny pointed hillocks. Because the degree of etching varies within a single emerald crystal, it is concluded that such samples were partially shielded from contact with other minerals of the natural assemblage from the etching fluid.

Conically developed emerald crystals, in general, show only growth layers related to basal and dipyramidal growth faces, but no prismatic growth sectors were developed in such crystals. The morphology of such samples resembles the basal growth sectors of Colombian trapiche emerald.

Emerald cups showing a skeletal rim with prismatic or dipyramidal faces forming its outer and inner surface reveal more or less deep indentations on the basal face. In some cases, the walls or rims form deep

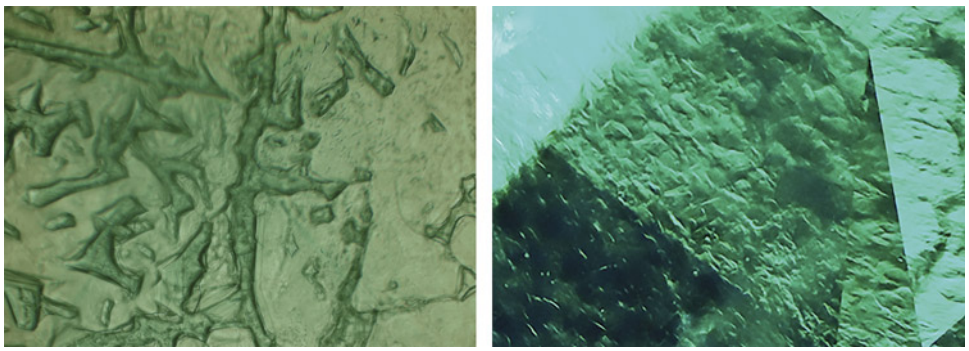

Figure 24. Patterns seen in faceted Colombian gota de aceite *emeralds display numerous irregular hillocks, columns, or walls. The left image is viewed in immersion, parallel to the* c*-axis. Photomicrographs by K. Schmetzer (left) and M.P.H. Curti, Bellerophon Gemlab (right); fields of view 1.9 mm (left) and 1.6 mm (right).*

cavities of prismatic or conical cups or even elongated central tubes within the crystal. Within the cavities of these cups, starting from a basal plane growth layer, we observe tiny columns or pyramidal crystallites, which frequently end in small basal faces. If such surface structures are overgrown subsequently with new emerald, the final result would show a crystal with an internal growth structure containing an inclusion pattern resembling the pattern described as *gota de aceite* in Colombian emerald.

ABOUT THE AUTHORS

Dr. Karl Schmetzer is an independent researcher living in Petershausen, near Munich. Gérard Martayan is a senior geophysicist and longtime emerald aficionado residing in Paris.

ACKNOWLEDGMENTS

The authors are grateful to Professor H.A. Gilg and N. Preisinger for their help with X-ray diffraction, X-ray fluorescence, and Raman spectroscopy to identify the cavity fillings in one sample. We are also grateful for numerous helpful comments and suggestions of the three peer reviewers of this manuscript.

REFERENCES

Arzruni A. (1894) Ein Beryllkrystall mit rhomboëdrischer Ausbildung. *Verhandlungen der Russisch-Kaiserlichen Mineralogischen Gesellschaft zu St. Petersburg*, Zweite Serie, Vol. 31, pp. 155–160.

Bartoshinsky Z.V., Matkovsky O.I., Srebrodolsky B.I. (1969) Accessory beryl from chambered pegmatites of the Ukraine. *Mineralogical Sbornik (Mineralogicheskii Sbornik)*, Vol. 23, No. 4, pp. 382–397 [in Russian].

Bernauer F. (1926) Die sog. Smaragddrillinge von Muzo und ihre optischen Anomalien. *Neues Jahrbuch für Mineralogie, Geologie und Paläontologie*, Supplemental Volume 54, pp. 205–242.

Beus A.A. (1966) *Geochemistry of Beryllium and Genetic Types of Beryllium Deposits*. W.H. Freeman and Company, San Francisco.

Bosshart G. (1991) Emeralds from Colombia (Part 2). *Journal of Gemmology*, Vol. 22, No. 7, pp. 409–425.

Demianets L.N., Ivanov-Shitz A.K., Gainutdinov R.V. (2006) Hydrothermal growth of beryl single crystals and morphology of their singular faces. *Inorganic Materials*, Vol. 42, No. 9, pp. 989–995, http://dx.doi.org/10.1134/S0020168506090111

Dem'yanets L.N., Ivanov-Schitz A.K. (2009) Beryl: Regeneration crystal growth and morphology of regeneration surfaces. *Journal of Surface Investigation. X-ray, Synchrotron and Neutron Techniques*, Vol. 3, No. 6, pp. 881–887, http://dx.doi.org/10.1134/S1027451009060068

Feklichev V.G. (1963) Microcrystalline morphology and investigation of the phenomena of solution of beryllium crystals. *Trudi Institut Mineralogii, Geochimii i Kristallochimii Redkich Elementov*, Akademija Nauk SSSR, Vol. 18, pp. 85–106 [in Russian].

Ford W.E. (1906) Some interesting beryl crystals and their associations. *American Journal of Science*, Vol. 22, No. 129, pp. 217–223.

Gao Y., Ng M., Carmona C., Lin Q. (2017) "Gota de aceite" effect in emerald: Observation and cause. *Gems & Technology Conference, Beijing*, pp. 95–97.

Goldschmidt V. (1913) *Atlas der Krystallformen, Band I*. Carl Winters. Universitätsbuchhandlung, Heidelberg, Germany.

Griffin L.J. (1951a) LXXIX. Microscopic studies on beryl crystals.–I. Observation of uni-molecular steps. *The London, Edinburgh, and Dublin Philosophical Magazine and Journal of Science*, Vol. 42, No. 330, pp. 775–786, http://dx.doi.org/10.1080/14786445108561306

——— (1951b) CXXXIII. Microscopic studies on beryl crystals.–II. Dislocations and the growth of {10$\bar{1}$0} prism faces. *London, Edinburgh, and Dublin Philosophical Magazine and Journal of Science*, Vol. 42, No. 335, pp. 1337–1352, http://dx.doi.org/10.1080/14786445108560951

Grigor'ev D.P. (1965) *Ontogeny of Minerals*. Israel Program for Scientific Translations Ltd., Jerusalem.

Gübelin E.J. (1944) Gemstone inclusions. *G&G*, Vol. 4, No. 12, pp. 174–179.

Gübelin E.J., Koivula J.I. (2008) *Photoatlas of Inclusions in Gemstones*, Volume 3. Opinio Publishers, Basel, Switzerland.

Hainschwang T. (2008) Extraordinary "gota de aceite" emerald submitted to the lab. *GEMLAB Research Newsletter,* Vol. 6.

Hills R.C. (1890) Etched beryls from Mount Antero, Colorado. *Proceedings of the Colorado Scientific Society*, Vol. 3, No. 2, pp. 191–192.

Himmel H., Schmidt-Zittel H. (1927) Wachstumsakzessorien am Beryll. *Zentralblatt für Mineralogie, Geologie und Paläontologie*, Abt. A., 1927, pp. 118–125.

Honess A.P. (1917) On the etching figures of beryl. *American Journal of Science*, Vol. 43, No. 255, pp. 223–236.

——— (1929) The theory of crystal etching and its significance in the classification of crystals. *Proceedings of the Pennsylvania Academy of Science*, Vol. 3, pp. 52–59.

Hunt T.S. (1892) *Systematic Mineralogy Based on a Natural Classification*, 2nd ed. The Scientific Publishing Co., New York.

Johnson P.W. (1961a) The Chivor emerald mine. *Journal of Gemmology*, Vol. 8, No. 4, pp. 126–152.

——— (1961b) All about emeralds – natural or synthetic. *Lapidary Journal,* Vol. 15, No. 1, pp. 118–131.

Johnston W.D. (1945) Beryl-tantalite pegmatites of Northeastern Brazil. *Bulletin of the Geological Society of America*, Vol. 56, No. 11, pp. 1015–1070, http://dx.doi.org/10.1130/0016-7606(1945)56[1015:BPONB]2.0.CO;2

Kiefert L., Schmetzer K. (1991) The microscopic determination of structural properties for the characterization of optical uniaxial natural and synthetic gemstones. Part 2: Examples for the applicability of structural features for the distinction of natural emerald from flux-grown and hydrothermally-grown synthetic emerald. *Journal of Gemmology*, Vol. 22, No. 7, pp. 427–438.

Klein F. (1941) *Smaragde unter dem Urwald*. Oswald Arnold Verlag, Berlin.

Kohlmann H. (1908) Beiträge zur Kenntnis des brasilianischen Berylls. *Neues Jahrbuch für Mineralogie, Geologie und Paläontologie*, Vol. 25 Supplement, pp. 135–181.

Koivula J.I. (1981) Etch figures on beryl. *Journal of Gemmology*, Vol. 21, No. 3, pp. 142–143.

von Kokscharow N. (Sohn) (1881) Beryll-Krystalle eines neuen Fundortes. *Bulletin de l'Académie Impériale des Sciences de*

St-Pétersbourg, Vol. 27, No. 1-7, pp. 35–38.
Kurumathoor R., Franz G. (2018) Etch pits on beryl as indicators of dissolution behaviour. *European Journal of Mineralogy*, Vol. 30, No. 1, pp. 107–124, http://dx.doi.org/10.1127/ejm/2018/0030-2703
Lacroix A. (1896) *Minéralogie de la France et de ses colonies*. Vol. 2, Librairie Polytechnique, Paris, pp. 8–22.
Lyckberg P., Chornousenko V., Wilson W.E. (2009) Famous mineral localities: Volodarsk-Volynski, Zhitomir Oblast, Ukraine. *Mineralogical Record*, Vol. 40, No. 6, pp. 473–506.
Medina J.A., Morante M., Leguey S. (1983) Natural etch pits in beryl related with the structure. *Bulletin de Minéralogie*, Vol. 106, No. 3, pp. 293–297, http://dx.doi.org/10.3406/bulmi.1983.7708
Moore T.P., Wilson W.E. (2016) The emerald mines of Colombia. *Mineralogical Record*, Vol. 47, No. 1, pp. 5–68.
Nassau K., Jackson K.A. (1970) Trapiche emeralds from Chivor and Muzo, Colombia. *American Mineralogist*, Vol. 55, No. 3-4, pp. 416–427.
Norton J.J., Page L.R., Brobst D.A. (1962) Geology of the Hugo pegmatite Keystone, South Dakota. U.S. Geological Survey Professional Paper 297-B, pp. 49–127.
Oishi S., Mochizuki K., Hirano S. (1994) Growth of emerald crystals by the flux evaporation method in MoO_3-B_2O_3 system. *Journal of the Ceramic Society of Japan*, Vol. 102, No. 1185, pp. 502–504, http://dx.doi.org/10.2109/jcersj.102.502 [in Japanese]
Penfield S.L. (1890) Some observations on the beryllium minerals from Mt. Antero, Colorado. *American Journal of Science*, Vol. 40, No. 240, pp. 488–491.
Penfield S.L., Sperry E.S. (1888) Mineralogical Notes: Beryl. *American Journal of Science*, Vol. 36, No. 215, pp. 317–320.
Petersson W. (1889) Om naturliga etsfigurer och andra lösningsfenomen på beryll från Mursinsk. *Bihang till Kongl. Svenska Vetenskaps-Akademiens Handlingar*, Afd. II, Vol. 15, No. 1, pp. 1–38.
Pignatelli I., Giuliani G., Ohnenstetter D., Agrosi G., Mathieu S., Morlot C., Branquet Y. (2015) Colombian trapiche emeralds: Recent advances in understanding their formation. *G&G*, Vol. 51, No. 3, pp. 222–259, http://dx.doi.org/10.5741/GEMS.51.3.222
Pignatelli I., Giuliani G., Morlot C., Salsi L., Martayan G. (2022) Colombian emerald oddities: Review and formation mechanisms. *Journal of Gemmology*, Vol. 38, No. 1, pp. 26–43.
Ringsrud R. (2008) *Gota de aceite*: Nomenclature for the finest Colombian emeralds. *G&G*, Vol. 44, No. 3, pp. 242–245, http://dx.doi.org/10.5741/GEMS.44.3.242
——— (2009) *Emeralds: A Passionate Guide*. Green View Press, Oxnard, California.
Sahama T.G. (1966) Polygonal growth of beryl. *Bulletin of the Geological Society of Finland*, Vol. 38, pp. 31–45.
Scandale E., Lucchesi S., Graziani G. (1990) Growth defects and growth marks in pegmatite beryls. *European Journal of Mineralogy*, Vol. 2, No. 3, pp. 305–312, http://dx.doi.org/10.1127/ejm/2/3/0305
Schmetzer K. (2009) A rare 'gota de aceite' Colombian emerald which had been treated. *Gems & Jewellery*, Vol. 18, No. 1, pp. 3–4.
——— (2019) Gem News International: Trapiche emerald from Colombia. *G&G*, Vol. 55, No. 1, pp. 156–158.
Schwarz D., Curti M. (2020) *Emerald: Modern Gemmology*. Bellerophon Gemlab Ltd, Paris and Bangkok.
Schwarz D., Giuliani G. (2002) South America: Colombia. In G. Giuliani et al., Eds., *Emeralds of the World*. extraLapis English No. 2. Lapis International, East Hampton, Connecticut, pp. 36–45.
Seager A.F. (1953) The surface structure of crystals. *Mineralogical Magazine*, Vol. 30, No. 220, pp. 1–25, http://dx.doi.org/10.1180/minmag.1953.030.220.02
Shaub B.M. (1937) Contemporaneous crystallization of beryl and albite vs. replacement. *American Mineralogist*, Vol. 22, No. 10, pp. 1045–1051.
Sinkankas J. (1981) *Emerald and Other Beryls*. Chilton Book Company, Radnor, Pennsylvania.
Smith J.S. (2021) From curio to designer gem…Rise of the trapiche. *Gems & Jewellery*, Vol. 30, No. 4, pp. 26–29.
Sun X., Gao Y. (2022) Gem Notes: Hexagonal growth structures displaying *gota de aceite* effect in Colombian emerald. *Journal of Gemmology*, Vol. 38, No. 1, pp. 11–12.
Sunagawa I. (1981) Characteristics of crystal growth in nature as seen from the morphology of mineral crystals. *Bulletin de Minéralogie*, Vol. 104, No. 2-3, pp. 81–87, http://dx.doi.org/10.3406/bulmi.1981.7438
——— (1999) Growth and morphology of crystals. *Forma*, Vol. 14, pp. 147–166.
——— (2003) Growth histories of mineral crystals as seen from their morphological features. In K. Byrappa and T. Ohachi, Eds., *Crystal Growth Technology*. Springer-Verlag, Berlin, Germany, pp. 1–23.
——— (2005) Minerals formed by vapor growth. In *Crystals: Growth, Morphology, and Perfection*. Cambridge University Press, Cambridge, UK, pp. 236–250.
Sunagawa I., Urano A. (1999) Beryl crystals from pegmatites: Morphology and mechanism of crystal growth. *Journal of Gemmology*, Vol. 26, No. 8, pp. 521–533.
Taube H. (1895/1896) Ueber die Aetzfiguren einiger Minerale. *Neues Jahrbuch für Mineralogie, Geologie und Paläontologie*, Supplemental Volume 10, pp. 454–469.
Tempesta G., Scandale E., Agrosi G. (2011) Striations and hollow channels in rounded beryl crystals. *Periodico di Mineralogia*, Vol. 79, No. 1, pp. 75–87, http://dx.doi.org/10.2451/2011PM0006
Tschermak G. (1897) *Lehrbuch der Mineralogie*. 5th edition, Alfred Hölder, Vienna, p. 147.
Vrba C. (1881) Smaragd von Sta Fé de Bogota. *Zeitschrift für Krystallographie und Mineralogie*, Vol. 5, No. 5, pp. 430–432.
Vrba C. (1895) Beryll von Pisek. *Zeitschrift für Krystallographie und Mineralogie*, Vol. 24, No. 1-2, pp. 104–112.
Weldon R., Ortiz J.G., Ottaway T. (2016) In Rainier's footsteps: Journey to the Chivor emerald mine. *G&G*, Vol. 52, No. 2, pp. 168–187, http://dx.doi.org/10.5741/GEMS.52.2.168
Zedlitz O. (1941) Goniometrische Untersuchungen der Lösungs- und Ätzerscheinungen an einem Beryllkristall von Minas Geraes, Brasilien. *Zentralblatt für Mineralogie, Geologie und Paläontologie, Abt. A*., pp. 98–108.